SYNDEPOSITIONAL TECTONIC ACTIVITY IN AN EPICONTINENTAL BASIN REVEALED BY DEFORMATION OF SUBAQUEOUS CARBONATE LAMINITES AND EVAPORITES: RED RIVER STRATA (UPPER ORDOVICIAN) OF SOUTHERN SASKATCHEWAN, CANADA

A Thesis Submitted to the College of
Graduate Studies and Research
In Partial Fulfillment of the Requirements
For the Degree of Master of Science
In the Department of Geological Sciences
University of Saskatchewan
Saskatoon

By
Hussam El Taki

PERMISSION TO USE

In presenting this thesis in partial fulfillment of the requirements for a Postgraduate degree from the University of Saskatchewan, I agree that the Libraries of this University may make it freely available for inspection. I further agree that permission for copying of this thesis in any manner, in whole or in part, for scholarly purposes may be granted by the professor or professors who supervised my thesis work or, in their absence, by the Head of the Department or the Dean of the College in which my thesis work was done. It is understood that any copying or publication or use of this thesis or parts thereof for financial gain shall not be allowed without my written permission. It is also understood that due recognition shall be given to me and to the University of Saskatchewan in any scholarly use which may be made of any material in my thesis.

Requests for permission to copy or to make other use of material in this thesis in whole or part should be addressed to:

Head of the Department of Geological Sciences
University of Saskatchewan
Saskatoon, Saskatchewan S7N 5E2

`

ABSTRACT

Late Ordovician Red River strata of southeastern Saskatchewan were deposited in a broad epicontinental sea. In the lower part, the Yeoman and Herald formations comprise two cycles of carbonate–evaporite sequences. Although these units possess an overall 'layer-cake' aspect, thickness variations especially in the Herald Formation show that accumulation was affected by syndepositional flexure, differential subsidence and displacement of fault-bounded blocks. The mainly laminated dolomudstones and anhydrites of the Lake Alma and Coronach members of the Herald Formation were deposited under relatively tranquil conditions. These units host different kinds of synsedimentary deformation features, interpreted to have been induced by earthquakes generated because of movements along basement faults thought to have been oriented orthogonally NE−SW and NW−SE. The low-energy environmental setting was conducive to preserving these features, referred to as 'seismites'.

The variety of seismites in the Herald Formation is related to the varying rheology of the carbonate or evaporite sediment, as well as shaking intensity. Brittle and quasi-brittle failure is represented by faults, microfaults, shear-vein arrays and pseudo-intraclastic breccias, mostly in dolomudstones which must have been stiff at the time of deformation. Plastic behaviour is recorded by soft-sediment deformation, comprising a family of features that includes loop bedding, folded laminae and convolute bedding. Indeed, these structures in enterolithic anhydrite are more reasonably interpreted as due to deformation than crystal growth, volume expansion and displacement, the more usual explanations. Sediment shrinkage and concomitant fluidization are recorded by dikelets containing injected carbonate mud or granular gypsum, the latter now preserved as anhydrite. Evidence for wholesale liquefaction, however, was not observed. These

rheological differences were caused by the primary nature of the sediment plus modifications due to early diagenesis and burial confinement. Shaking intensity is difficult to gauge, but it is presumed that a minimum of VI on the modified Mercalli scale was required to produce these features. Consequently, shaking of lesser magnitude was probably not recorded.

The geographic distribution of seismites should reflect the location of basement faults presumed to have been active during deposition, and indeed there is a concentration adjacent to the known location of syndepositonal fault lineaments. In addition, the stratigraphic distribution of seismites records higher frequencies of activity of these same faults. These distributions show that earthquake-induced ground motion was common during deposition of the Lake Alma Member in southeastern Saskatchewan but less so during deposition of the Coronach Member.

Seismites serve as proxies for the activity of relatively nearby syndepositional faults making up the tectonic fabric of sedimentary basins. They also point to basement features that, if re-activated, can induce fracture porosity or influence subsurface fluid flow. Syndepositional tectonism undoubtedly had a much more profound influence on many successions than is presently accepted, and its effects are more widespread than currently appreciated.

ACKNOWLEDGMENTS

I am grateful to Professor B.R. Pratt for suggesting and supervising this project and to Professors K. M. Ansdell and L. A. Buatois for serving as supervisory committee members. Also I am thankful to the staff of the Subsurface Geological Laboratory in Regina, especially F. M. Haidl, for granting us access to core under their care and for providing other location and stratigraphic data.

TABLE OF CONTENTS

PERMISSSION TO USE i

ABSTRACT.....ii

ACKNOWLEDGMENTS iv

TABLE OF CONTENTS.....v

LIST OF TABLES.....vii

LIST OF FIGURES viii

1. INTRODUCTION 1

2. METHODS 2

3. DEPOSITIONAL AND TECTONIC ENVIRONMENT.....3

4. RED RIVER STRATA.....8

4.1 HERALD FORMATION.....9

4.1.1 LAKE ALMA MEMBER.....9

4.1.2 CORONACH MEMBER.....9

5. SEISMITES 12

5.1 ORIGIN OF SEISMITES 12

5.2 SEISMITE TYPE.....14

5.2.1 DEFORMATION IN DOLOMUDSTONE.....14

5.2.2 DEFORMATION IN ANHYDRITE.....16

6. DISTRIBUTION OF SEISMITES 29

6.1 STRATGRAPHIC DISTRIBUTION 29

6.2 GEOGRAPHIC DISTRIBUTION.....31

7. CONCLUSIONS.....43

8. REFERENCES 45

9. APPENDICES 53

9.1 THIN SECTIONS 53

9.2 PUBLICATION 54

LIST OF TABLES

Table 1 Spatial distribution of seismite frequency in dolomudstone.....37
Table 2 Spatial distribution of seismite frequency in anhydrite 37

LIST OF FIGURES

Figure 1 Paleogeography reconstruction 5
Figure 2 Williston Basin 6
Figure 3 Location map and basement lineaments.....7
Figure 4 Lithostratigraphic nomenclature.....8
Figure 5 Idealized stratigraphy 10
Figure 6 Isopach maps 11
Figure 7 Classification of deformation features.....18
Figure 8 Soft-sediment deformation in dolomudstone 19
Figure 9 Soft-sediment deformation in dolomudstone 20
Figure 10 Molar-tooth structure in dolomudstone.....21
Figure 11 Quasi-brittle deformation in dolomudstone.....22
Figure 12 Soft-sediment and quasi-brittle deformation in dolomudstone 23
Figure 13 Quasi-brittle deformation in dolomudstone.....24
Figure 14 Brittle failure in dolomudstone.....25
Figure 15 Soft-sediment deformation in anhydrite.....26
Figure 16 Soft-sediment deformation in anhydrite.....27
Figure 17 Quasi-brittle deformations in anhydrite.....28
Figure 18 Cross-section A-A^1.....33
Figure 19 Cross-section B-B^1 34
Figure 20 Cross-section C-C^1 35
Figure 21 Cross-section D-D^1.....36
Figure 22 Map of ratio of soft-sediment deformation versus brittle failure 38
Figure 23 Graph of numbers of soft-sediment and quasi-brittle deformation 39

Figure 24 Isopleth map of seismites in the Lake Alma and Coronach members combined 40

Figure 25 Isopleth map of seismites in Lake Alma Member.....41

Figure 26 Map of lineaments and seismite frequency 42

INTRODUCTION

In recent years sedimentologists have become increasingly aware of the widespread occurrence in marine and lacustrine sedimentary rocks of deformation features attributable to syndepositional earthquake-induced shaking. Commonly referred to as 'seismites', the great variety of such features was dictated by shaking intensity and the rheology of the sediment on the sea or lake floor and under shallow burial. Rheology is controlled by the size and shape of the sedimentary particles, degree of cementation by authigenic minerals, presence and nature of organic matter, water content and amount of burial. Deformation ranges from brittle and quasi-brittle to plastic, to loss of shear strength and convolution, to dewatering coupled with sediment injection. They typically record complex stresses that arise during protracted ground motion. After a certain burial depth, the confining pressure exerted by the enclosing sediment prevents deformation. Hitherto often ascribed to gravitational slumping or evaporite solution–collapse, seismites do not require a slope or cavity to form.

In rare instances, a paleo-fault and its directly associated deformed sediment may be exposed (e.g. Rodríguez-Lopez et al., 2007). In other cases, seismites can be related to specific nearby faults (e.g. Rossetti and Góes, 2000; Kahle and Onasch, 2002; Paz and Rossetti, 2005; Fortuin and Dabrio, 2008). The episodic movement along known or approximated fault zones can be detected by the frequency of seismites recorded in stratigraphic sections (e.g. Pratt, 1994, 1998a; Migowski et al., 2004; Weidlich and Bernecker, 2004). Usually, however, it is not possible to relate seismites to individual tectonic elements because the limitations of exposure

leave their location unknown, or the ground motion was generated by fault movement far from the locality under study.

The subsurface should be a good laboratory to explore the stratigraphic record of synsedimentary faulting, provided that well density and core coverage is sufficient, because it can be integrated with the tectonic fabric of the basin as revealed by seismic imaging. It appears, however, that this opportunity has yet to be exploited. With this in mind, Late Ordovician Red River strata in southeastern Saskatchewan were selected for study (El Taki and Pratt, 2009), because laminated dolomites and anhydrites of the Herald Formation were known to exhibit a variety of seismites (Pratt and Haidl, 2008). This study documents the nature, stratigraphic occurrence and geographic distribution of seismites in this unit and uses them as a proxy for determining the timing and magnitude of earthquake events along nearby basement faults. It shows that indeed seismites serve as a window on the tectonic behaviour of a basin even, as in this case, in the middle of a broad, shallow epicontinental sea.

METHODS

The study area extends across townships 1−17 and ranges 1−24W2 of southeastern Saskatchewan, chosen because of core availability, the prior identification of synsedimentary deformation features in the Herald Formation (Pratt and Haidl, 2008), and its underlying basement tectonic fabric of vertical faults believed to have been active during the Cambrian and Ordovician (Kreis and Kent 2000). Almost all available cores in the Herald Formation were examined, which totalled those of 65 wells. This sample size includes 43 complete cores through

the Lake Alma Member, and 22 through the lower portion of the Coronach Member. Thus, coverage of the latter unit is limited. Slabbed core surfaces were examined with the aid of a 10X hand lens and binocular microscope. More than 50 samples were collected for petrographical study.

Historically well locations were drilled mostly to test structural traps in the Yeoman Formation revealed by seismic imaging. Thus, wells are distributed preferentially on or nearby structural lineaments. Although in theory this represents an unavoidable geographic bias, density of coverage is still relatively high across the study area.

The variety of deformation features is described and interpreted in terms of the rheological properties of the sediments on and just below the sea floor. Stratigraphic cross-sections are prepared and deformed horizons correlated on the basis of lithological markers and estimated equivalence. Isopleth maps show geographically the relative abundance of deformation features.

DEPOSITIONAL AND TECTONIC ENVIRONMENT

During the Cambrian and Ordovician different phases of tension and collision created by plate motion resulted in multiple phases of epeirogenic flexure, block movement and lateral displacement in the interior of Laurentia (Figure 1). Local downwarping and upwarping along basement faults have been one of the main factors that affected sedimentation patterns within epicontinental platforms. The Williston Basin is an intracratonic sag basin in the center of the

craton. Overall sedimentation in the basin was controlled by local as well as regional fault systems which were later reactivated (Oglesby, 1987; Lefever *et al.*, 1987; Greggs and Greggs, 1989, Gerhard *et al.*, 1991). In southeastern Saskatchewan the basement appears to have been dissected by a series of lineaments dominated by an orthogonal NW−SE and NE−SW orientation (Porter and Onge, 1991). Three to four basement lineaments have been recognized in this area: the Cedoux–Midale trend, Montmartre–Weir Hill trend and the Brockton–Froid lineaments (Figure 3; Nimegeers and Haidl, 2004).

In general, thickening of Red River strata in the centre of the Williston Basin can be ascribed to greater subsidence (Figure 2; Kendall, 1976). Local variation in thickness indicates that structural elements were variably active during deposition (Kreis and Haidl in Kries *et al.*, 2004). The Lake Alma anhydrite unit is present over the entire study area, ranging from 3 m to 7.5 m in thickness, with pronounced variation over short distances (Pratt and Haidl, 2008) that may be due to differential subsidence or solution–collapse due to partial removal of the anhydrite about the same basement structural elements. By contrast, the Coronach anhydrite unit is less geographically widespread and occurs only in the southern and south-western portion of the study area. The uniform thickness of the Yeoman Formation, however, implies that basement faulting was essentially inactive during the early phase of deposition.

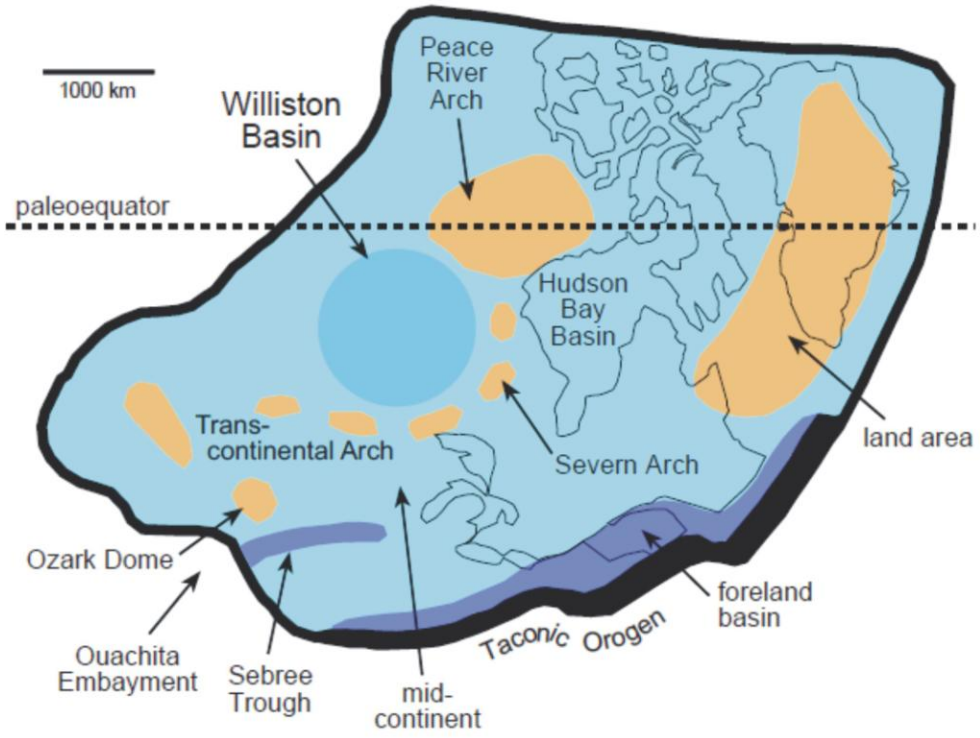

Fig.1. Paleogeographic reconstruction showing the location of the Williston Basin with the distribution of Edenian and Maysvillian (Late Ordovician) major structural features (From Pratt and Haidl, 2008)

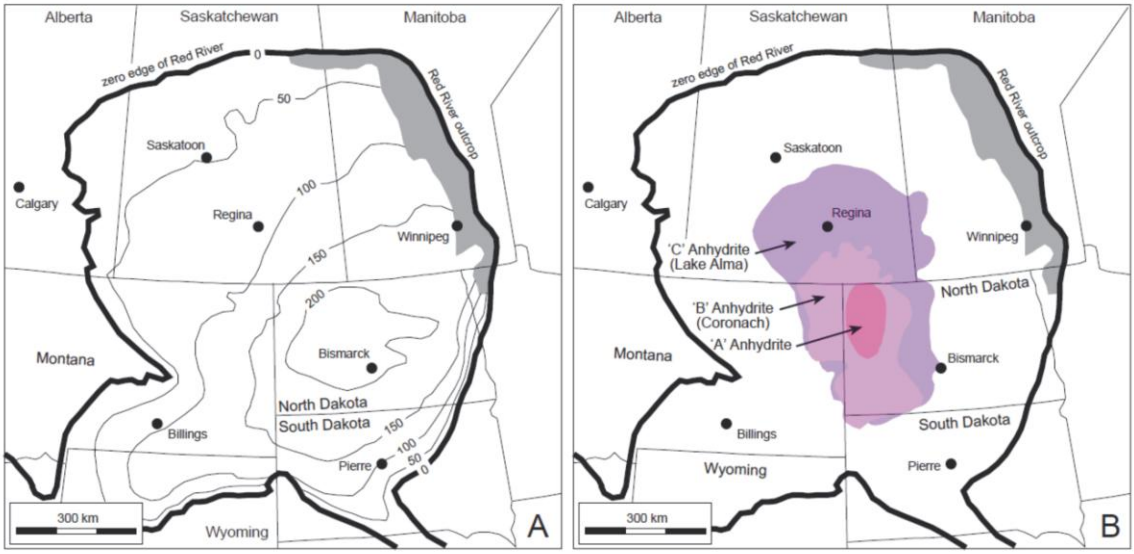

Fig.2. (A) Map of central Williston Basin showing the depocenter of Red River strata east of Bismarck, North Dakota (B) Distribution of the Red River strata and correlatives, with its three successive anhydrite units. (From Pratt and Haidl, 2008)

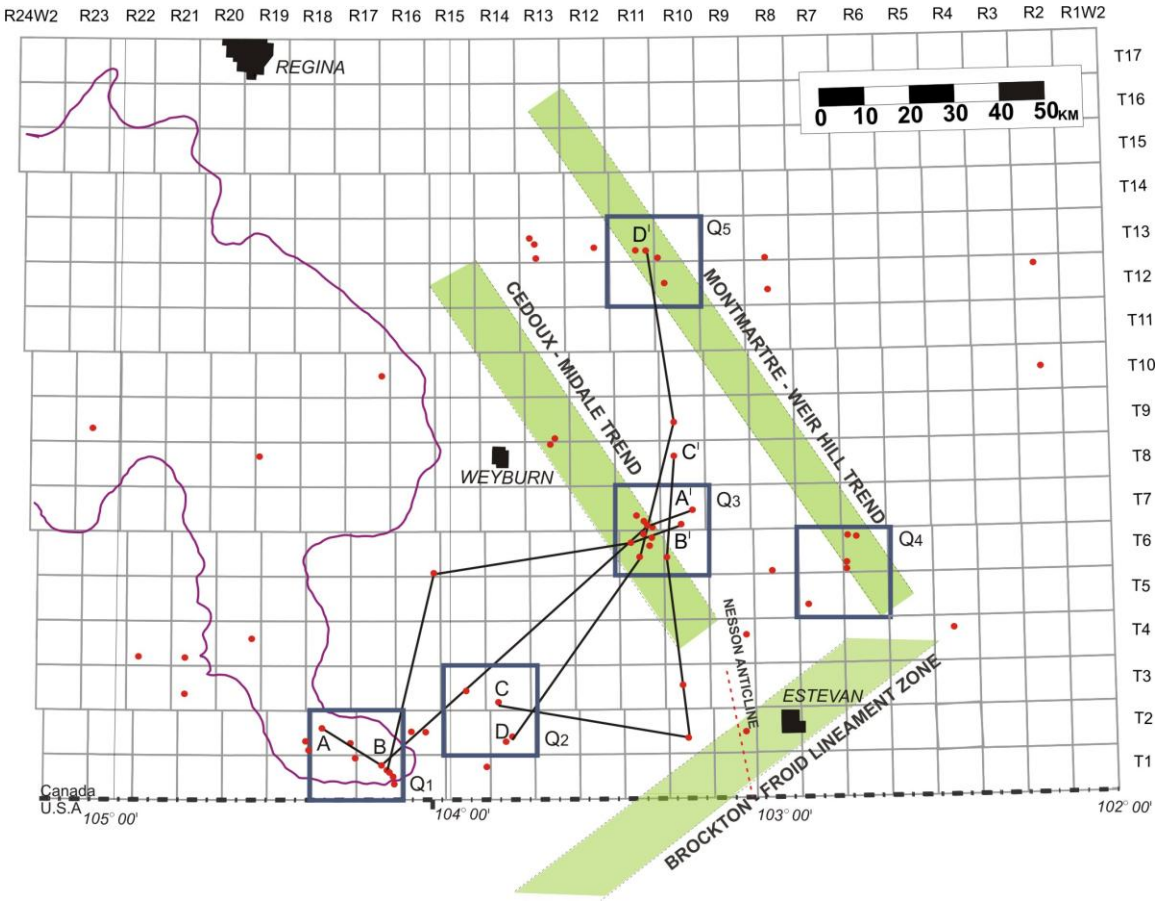

Fig.3. Location map of the study area in SE Saskatchewan showing the position of examined wells (red dots) and cross-sections A–A', B–B', C–C' in Figures 18–20. The five outlined boxes are quadrants Q1, Q2, Q3, Q4 and Q5 used for relating deformation to nearby fault activity. Three green bands are trends of linear basement structures. Also shown by a dotted red line east of Estevan is the northern extension of the Nesson Anticline. The purple line delineates the area of total dissolution of the Middle Devonian Prairie Evaporite; the Hummingbird trough occupies the southern part of this area. (Modified from Nimegeer and Haidl, 2004)

RED RIVER STRATA

The Late Ordovician succession comprising Red River strata (Fig. 4), which forms part of the Tippecanoe sequence, exhibits a series of large-scale shallowing upward or 'brining-upward' cycles of limestone, dolomite and anhydrite (Longman and Haidl, 1996; Pratt and Haidl, 2008; Fig.5). These carbonate–evaporite cycles were deposited in an intracratonic basin where an epeiric platform setting has prevailed. Anhydrite units accumulated in the inner central area of the restricted parts of the carbonate platform (Longman and Haidl, 1996). Fossiliferous bioturbated wackstone, packestone and locally grainstone units, on the other hand, were deposited under open-marine setting where laminated dolomitized lime mudstone intervals were deposited in a relatively subtidal shallow low-energy environment. But increased water temperatures and salinity may have been important factors for the rarity of fauna and bioturbation in is facies (Pratt and Haidl, 2008).

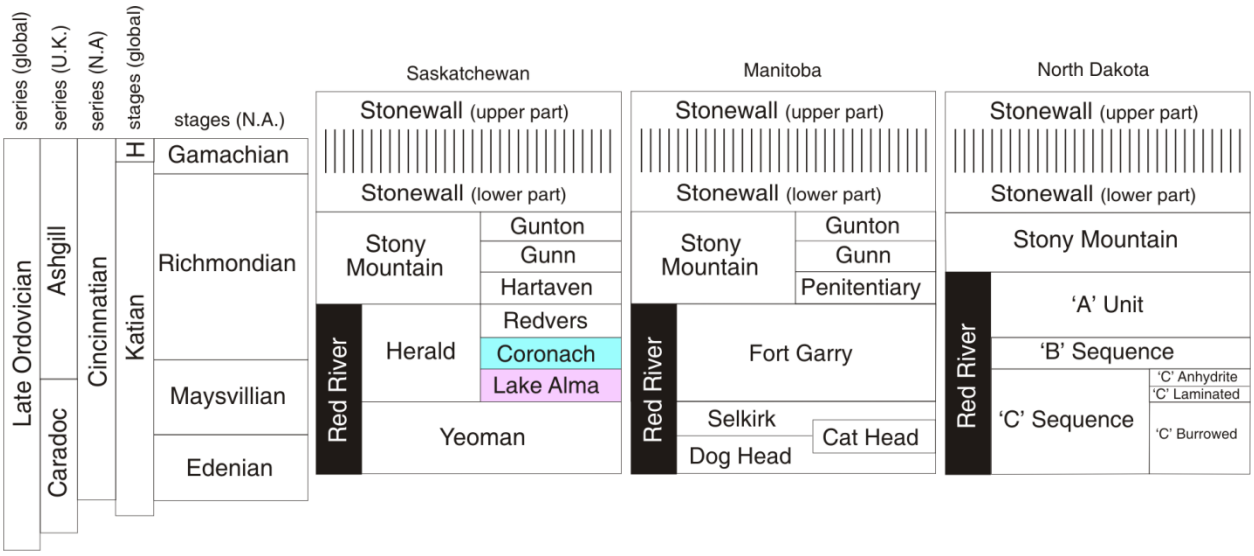

Fig.4. Lithostratigraphic nomenclature of the Red River, Stony Mountain and Stonewall strata in Saskatchewan, Manitoba and North Dakota. The Lake Alma and Coronach members comprise the lower part of the Herald Formation. Global stages after Bergström et al. (2009). (Modified from Pratt and Haidl, 2008.)

Herald Formation

The Herald Formation is about 35 m thick and is subdivided into three successive members: the Lake Alma, Coronach and Redvers, the lower two being the focus of this study (Figure 5).

Lake Alma Member

Abruptly diminished bioclastic content and bioturbation occurs at the transition from the Yeoman Formation into the basal Lake Alma Member. The transition is marked typically by planar to cross laminating passing upward into more massive laminated dolomudstones. Peloidal dolograinstone occurs locally at the base. This unit is about 10 m thick. The dolomudstone is overlain by two laminated to enterolithic anhydrite units with an intervening laminated dolomudstone, informally termed the upper Lake Alma Member can reach a thickness of 6.5 m (Figure 6A).

Coronach Member

The Coronach Member can be split into four informal units (Urban and Qing, 2007). The basal part is a uniformly 1.5 m thick bed composed of laminated argillaceous dolomudstone. Above is a thicker unit of moderately burrow-mottled packstones and wackestones that reaches a maximum thickness of 10 m. This is capped in turn by a unit of dolomudstone and then laminated to nodular and enterolithic anhydrite (Fig.6B).

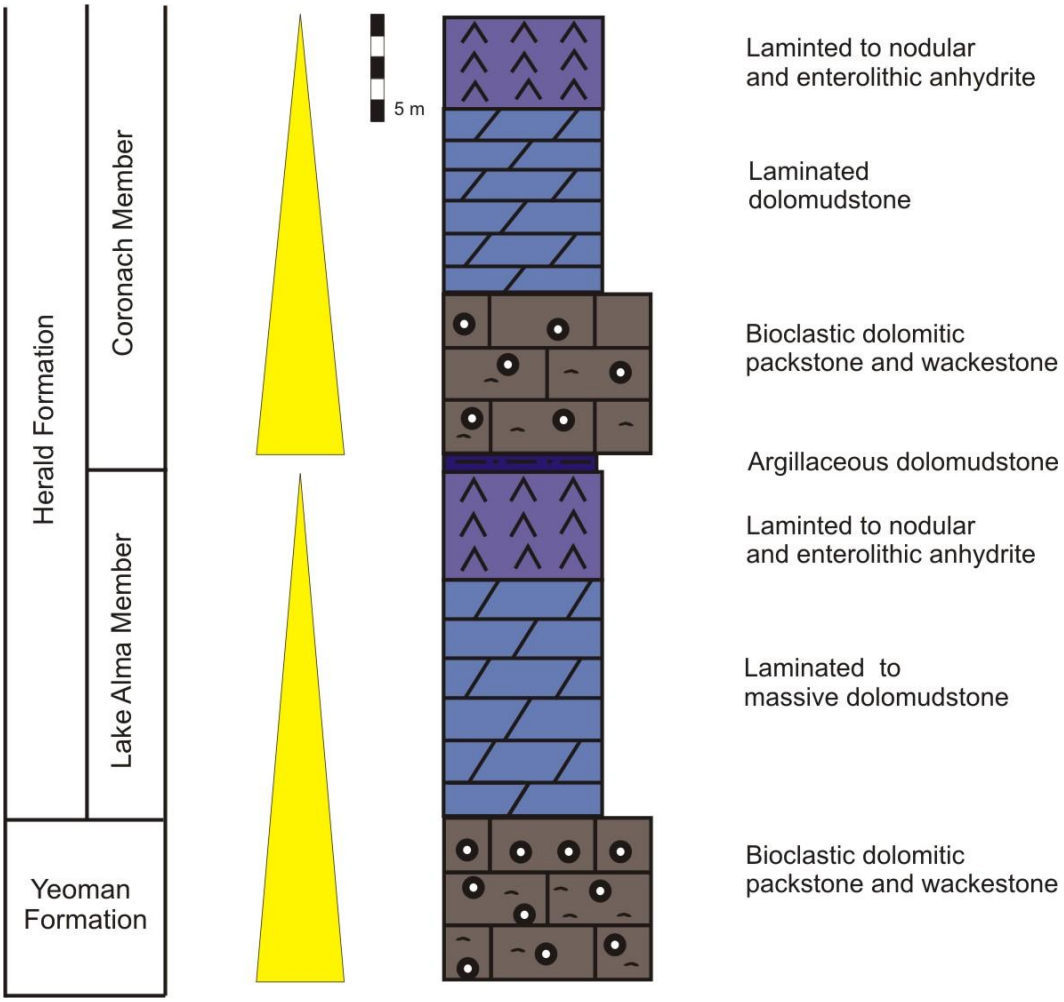

Fig.5. Shallowing-or brining-upward successions in the Red River strata. Yellow triangles depict the shallowing upward trend.

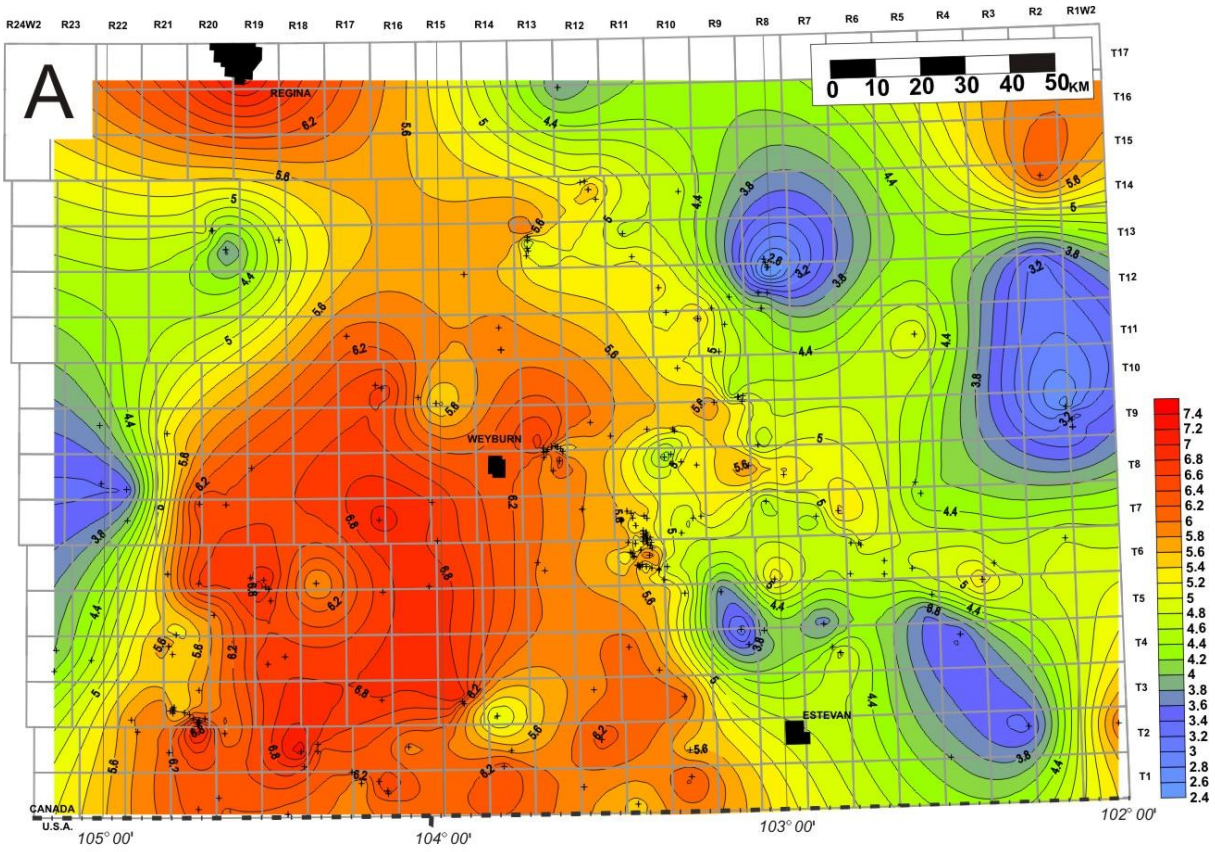
A
R24W2 R23 R22 R21 R20 R19 R18 R17 R16 R15 R14 R13 R12 R11 R10 R9 R8 R7 R6 R5 R4 R3 R2 R1W2
T17 T16 T15 T14 T13 T12 T11 T10 T9 T8 T7 T6 T5 T4 T3 T2 T1
0 10 20 30 40 50KM
REGINA
WEYBURN
ESTEVAN
CANADA
U.S.A.
105° 00'
104° 00'
103° 00'
102° 00'
7.4 7.2 7 6.8 6.6 6.4 6.2 6 5.8 5.6 5.4 5.2 5 4.8 4.6 4.4 4.2 4 3.8 3.6 3.4 3.2 3 2.8 2.6 2.4

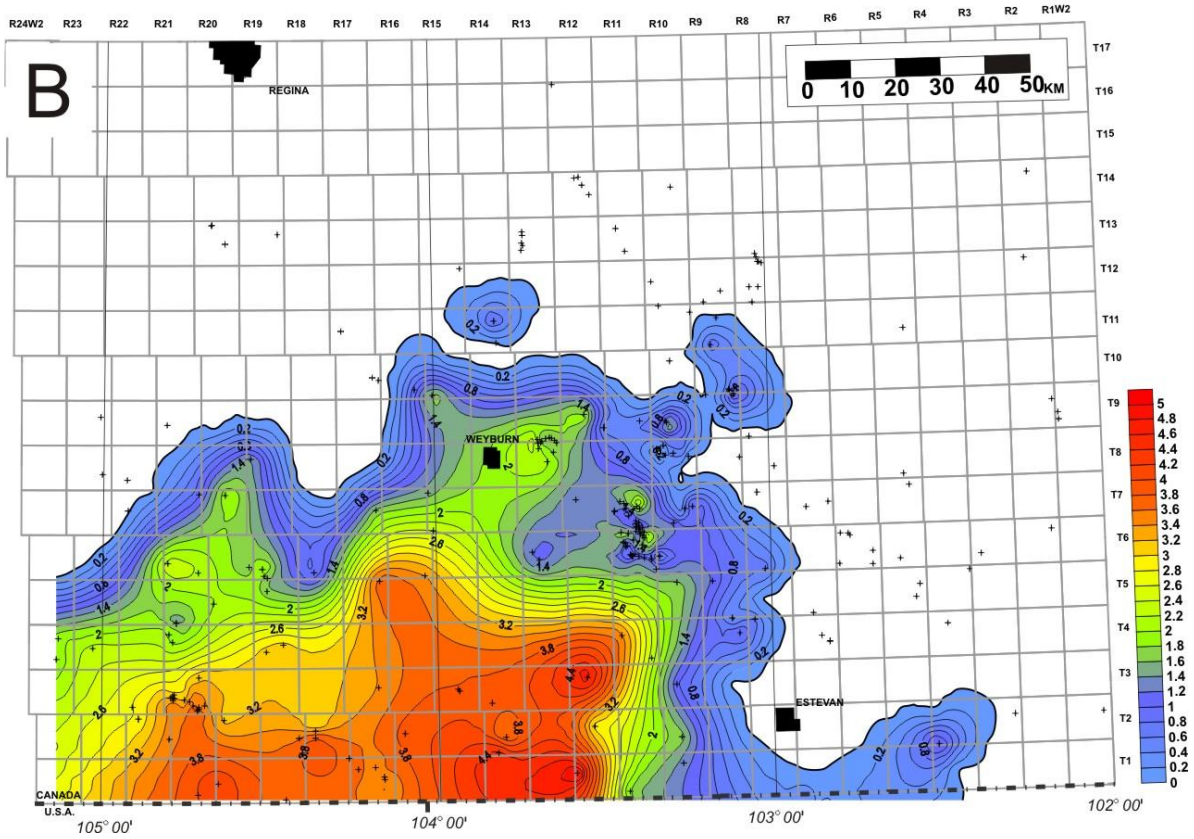
B
R24W2 R23 R22 R21 R20 R19 R18 R17 R16 R15 R14 R13 R12 R11 R10 R9 R8 R7 R6 R5 R4 R3 R2 R1W2
T17 T16 T15 T14 T13 T12 T11 T10 T9 T8 T7 T6 T5 T4 T3 T2 T1
0 10 20 30 40 50KM
REGINA
WEYBURN
ESTEVAN
CANADA
U.S.A.
105° 00'
104° 00'
103° 00'
102° 00'
5 4.8 4.6 4.4 4.2 4 3.8 3.6 3.4 3.2 3 2.8 2.6 2.4 2.2 2 1.8 1.6 1.4 1.2 1 0.8 0.6 0.4 0.2 0

Fig.6. Isopach maps of anhydrite intervals. (A) Upper Lake Alma Member. (B) Upper Coronach Member. Contour interval 0.2 m. (Modified from Nimegeers and Haidl, 2004.)

SEISMITES

Origin of Seismites

During deposition, surface and near surface sediments will respond to earthquake-induced shaking by mechanical deformation in a variety of different forms that varies from soft and plastic to quasi-brittle deformation and brittle failure. Seismically related deformation features are ascribed to earthquake magnitudes of at least 5 to 5.5 (Sims, 1973; Allen, 1986). Deformation structures were cautiously introduced at first for relating sediment deformation at the time of earthquake-induced shock and shaking events (Seilacher, 1967, 1984; Sims, 1973). In unlithified sediments, seismogenic deformation features of different morphologies are now seen to include convolute bedding, loop bedding and sandstone dykes (Montenat *et al*., 2007), as well as deformation bands in sandstones (Fossen *et al.*, 2007). Some of these features form due to overloading from both dewatering and escape structures (Moretti and Sabato 2007), whereas others which get plastically deformed are explained as by simultaneous shrinkage and injection of granular sediment into cracks, producing features that have been referred to ‘syneresis cracks’ and molar-tooth structure (Pratt 1998a, 1998b).

Seismically related deformation features of different scales show a relationship to faulting and its activity. For example, large-scale syn-sedimentary structures appearing on the

surface like ball and-pillow, load and dyke features originate due to earthquake-induced stresses related to nearby faults (Moretti *et al.*, 2002; Fortuin and Dabrio, 2008). However, the stratigraphic distribution of seismites in between undisturbed layers records seismotectonic events and activity through time (Sims, 1973; El-Isa and Mustafa, 1986; Pratt, 1994, Marco and Agnon, 2005). This approach is also used in studying sediment deformation for the reconstruction of tectonic effects within basins (Pratt 1998, 2001a; Onasch and Kahle 2002; Moretti, 2000).

Deformation features caused by forces other than seismic shaking, like slumps, microfaults, convolute bedding, overturned crossbedding, clastic dykes and sand volcanoes, could be related to physical conditions acting upon sediments at the time of deposition. Deformation can be triggered by gravitational drag, unequal confining pressure forces and circulating fluid movement (Maltman, 1984; Owen 1987, 1995; Plaziat *et al*., 1990) in unconsolidated and consolidated sediments that can be caused by mechanical processes such as loading, liquefaction and fluidization. Therefore, in many cases, interpreting the origin of deformation in sediments has been typically considered a controversial issue (Kirkland and Anderson, 1970; Owen, 1996, Ortner 2007, Simms, 2006) which may or may not tentatively disclose a relationship to seismicity.

In the Herald Formation, deformation features are seismically related or induced, since they are small-scale and are sporadically widespread in large numbers. Usually if the carbonate ramp has a much steeper slope, then local mass movement and debris flows might be triggered. This is unlikely for the carbonate and evaporite sediments that have been deposited on a nearly flat bottomed epeiric carbonate platform under low-energy environmental conditions. Moreover,

in times of seaway restriction and gradually rising water temperatures, viscosity hugging bottom brines were also not a factor for deforming sediments throughout syn-deposition of gypsum.

Seismite Type

Deformation in Dolomudstone

A variety of deformation features ascribed to earthquake-induced ground motion is recognized in the carbonate and anhydrite units (Figure 7). These seismites reflect the rheology of the sediment at the time of the event as well as the magnitude of the event. The thickness of a deformed interval does not surpass 0.2 m and may encompass more than one seismite. Naturally, to some extent these are intergradational. For example pseudobreccia may intergrade with microfaulted domains. The superposition of events in a single earthquake and the difference in rheological change at the time of burial from soft to stiff can occur within the same interval.

Soft or plastic sediment deformation is recognized in dolomudstones where it shows a spectrum of deformation styles from disrupted plane to wavy laminae, intercalated loop bedding, convolute bedding and injection dikelets consisting of laterally folded recumbent laminae. Folded and disrupted laminae show disruption in different attitudes from short wiggly folds to tightly recumbent and highly convoluted and overturned folds in laminated dolomudstone (Figure 8A and B). Loop bedding consists of rounded balls of dolomudstone interconnected in a beed-like shaped form which is sandwiched in between two stiffer layers (Figure 8C and D;

ElTaki and Pratt, 2009, figure 6B). These structures also show thicker bundled loop features or microboudins (Figure 9A and B; Pratt and Haidl, 2009, figure 8A).

Molar-tooth structure is represented by folded, buckled and then smeared mudstone-filled dikelets in dolomudstones (Figure 10A and 10B; El Taki and Pratt, 2009, figure 6A). It is restricted to the basal part of the Coronach Member (Figure 18; El Taki and Pratt, 2009, figure 8).

Convolute bedding involves plastic deformation and folding of shallow buried sediments. Loop bedding in dolomudstone laminae is initiated by back and forth motion which disrupts softer layers hosted in stiffer thinly bedded laminae by plastically deforming them into interconnected ball up structures “loops”. Mudstone-filled dikelets are generated when seismic shaking induces the liquefaction of sediment and loss of cohesive strength to force equant mud-sized particles to be injected into dewatering-induced shrinkage cracks (Pratt, 1998b).

Quasi-brittle and brittle failure in laminated and massive dolomudstone forms in the Lake Alma and Coronach members as pseudo-breccia, en-échelon shear vein arrays, microfaults and cracks (Figure 7). Pseudo-cataclastic features of detached, twisted and disrupted dolomudstone laminae form pseudo-intraclast breccia (Figure 11A-C). In interbedded mudstone these features are minor but are clearly seen in thin section alongside microfolds and buckled laminae (Figure 12A-D; Pratt and Haidl, 2009, figure 8C). Boudinage features are also accompanied by squeezed sediment in between nodules or previously opened cracks (Figure 11D). En-échelon shear veins are another form of quasi-brittle failure. These vein structures occur as a splay of straight to

obliquely branching arrays (Figure 13A-C; El Taki and Pratt, 2009, figure 5A). On the other hand, brittle failures consist of microfaults and cracks. Microfaults range from low-angle thrust-like microfaults and normal faults (Figure 14A and B; Pratt and Haidl, figure 8D) whereas cracks exhibit zigzag shaped features (Figure 14B).

Quasi-brittle deformation features form in response to deformation processes in between the soft, plastic and brittle domains. While vein arrays indicate only shearing forces that disrupt dolomudstone in arrays, pseudo-cataclasis involves tensional as well as shearing forces that disrupt and detach thicker laminae and massive dolomudstone. Brittle features are a result of type I fracturing caused by sliding as a consequence of tensional and compressional stresses which leads to intrastratal disruption with clay-filled cracks. Also where obliquely oriented shear veins are present with intraclast-like breccia, it suggests interbedding of sediments of varying rheology, from soft to stiff, such that some had more cohesiveness and resisted failure than other sediment layers which were fragile and broke along bedding planes.

Deformation in Anhydrite

Soft-sediment deformation in anhydrites occurs as folded laminae and loop bedding, horizontally to vertically sheared and disrupted irregular nodules, as well as injecting dikelets that displace nodular anhydrite (Figure 7).

Adjacent, undeformed primary lamination (Figure 15B) suggests that there were no rheological differences over the deformed interval. On the contrary, due to the enterolithic nature

of nodular anhydrite (Figure 15A) deformation as in convolute bedding are difficult to discern. Microfolding in laminated and nodular anhydrites occurs as lateral short and long parallel sets of horizontal wavy microfolds (Figure 15C and D; El Taki and Pratt, 2009, figure 7A). Along grain contact boundaries chunks of anhydrite laminae ball up into loop-like features. Similarly along bedding planes softer individual laminae get detached from the adjacent boundaries (Figure 15C). On the other hand, dikelets in anhydrites are oriented nearly vertically and form wavy injection configurations similarly to molar-tooth structure in dolomudstone (Figure 16A and B; El Taki and Pratt, 2009, figure 7B). Quasi-brittle deformation in anhydrite shows pseudobreccia-like features (Figure 17A), some of which are moderately disrupted into a vertically array of boudins (Figure 17B).

Soft to quasi-brittle deformation in anhydrite took place during the early phases of gypsum deposition. Microfolding is formed when gypsum plastically flows during the shaking motion of an earthquake. Micro-dikelets are presumed to have formed under continous injection phases of granular gypsum and small amounts of carbonate mud into spaces formed by shrinkage and dewatering of gypsum. Some are more cohesive and deformed by quasi-brittle deformation and were detached and disrupted in response to cataclasis.

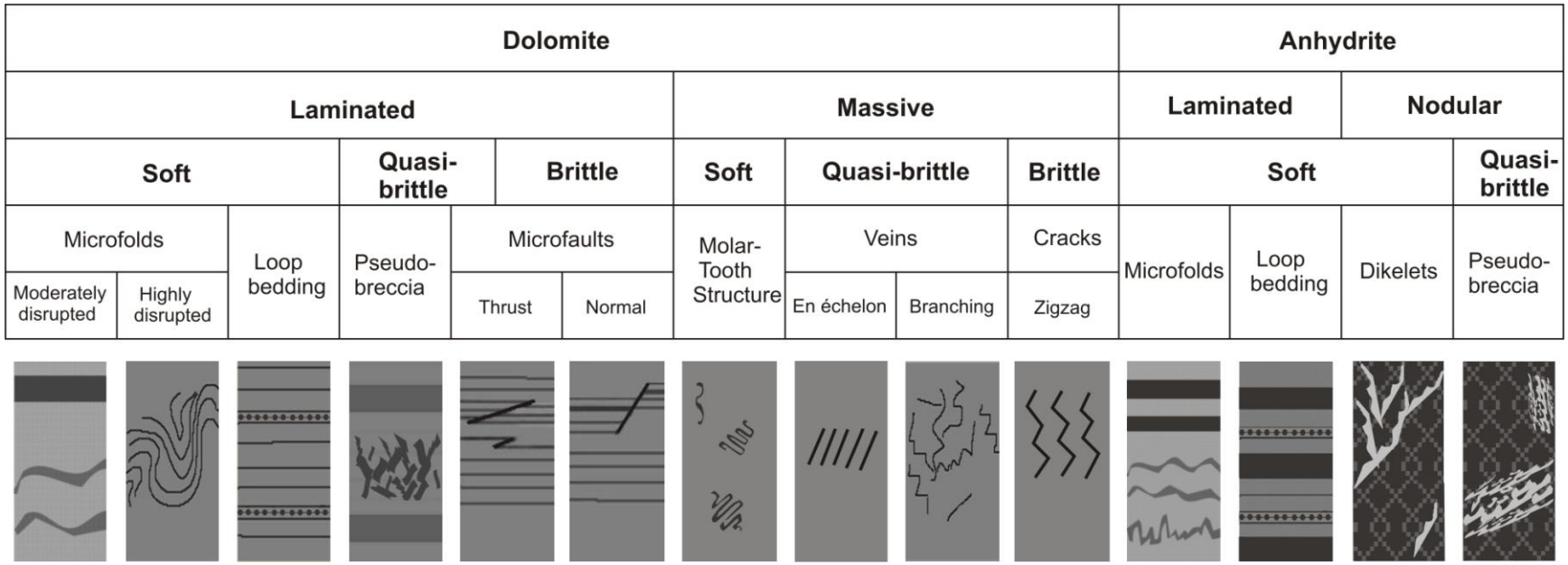

Fig.7. Classification of deformation features identified in dolomudstone and anhydrite of the Coronach and Lake Alma members.

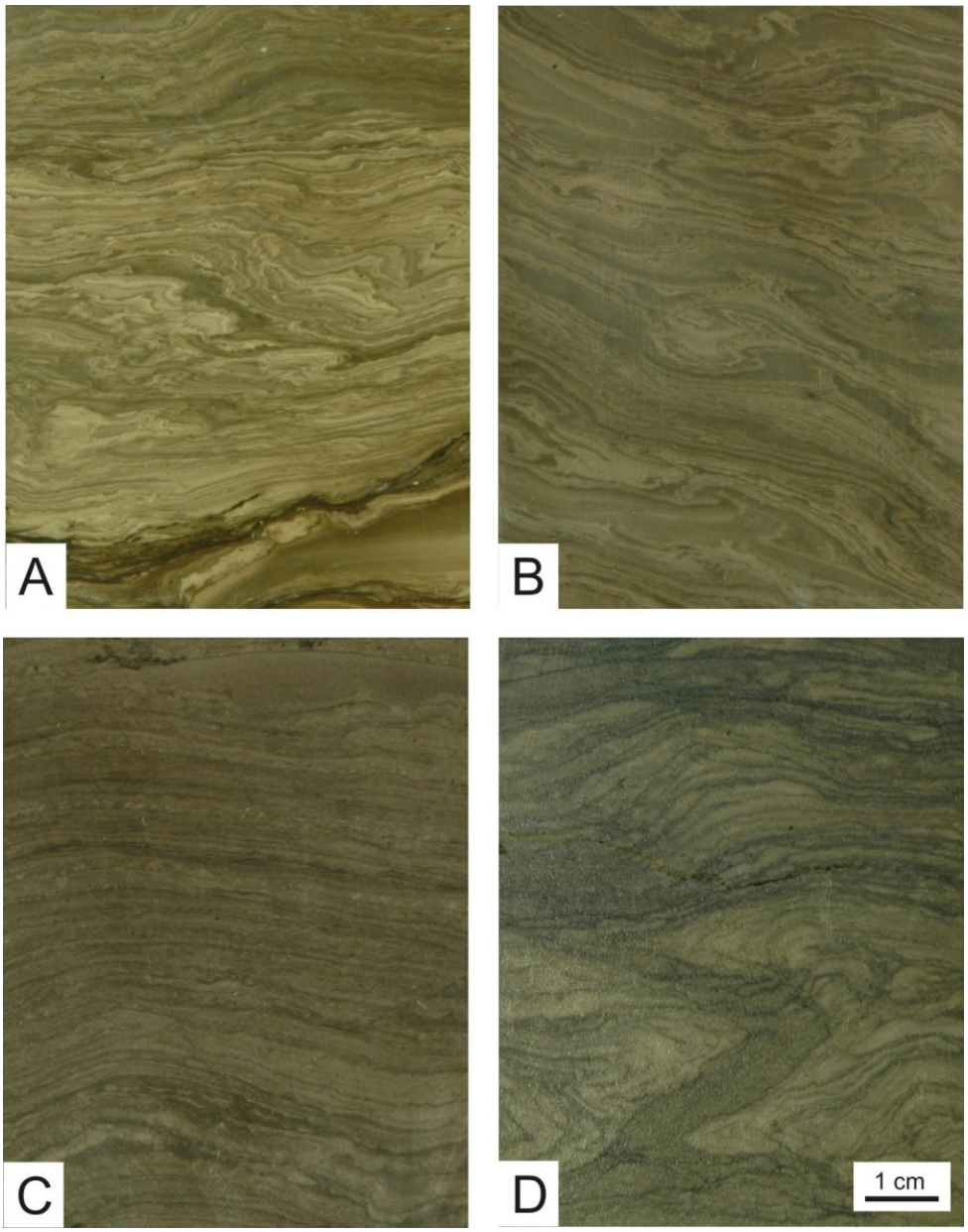

Fig.8. Vertically oriented slabbed cores of laminated dolomudstone with soft-sediment deformation; scale bar same for all. A) Convolute bedding consisting of laterally microfolded laminae and mudstone-filled dikelets. Lower Lake Alma Member, 07-16-06-11W2, 2591.5 m. B) Convolute bedding of laminated dolomudstone laminae. Upper Lake Alma Member, 06-04-06-08W2, 2630 m. C) Undeformed plane and wavy laminae with intercalated loop bedding, Lower

Lake Alma Member, 16-23-04-09W2, 2749 m. D) Vertically folded mudstone-filled dikelet in undeformed plane and wavy laminae with intercalated loop bedding. Basal Coronach Member, 15-09-02-14W2, 3030 m.

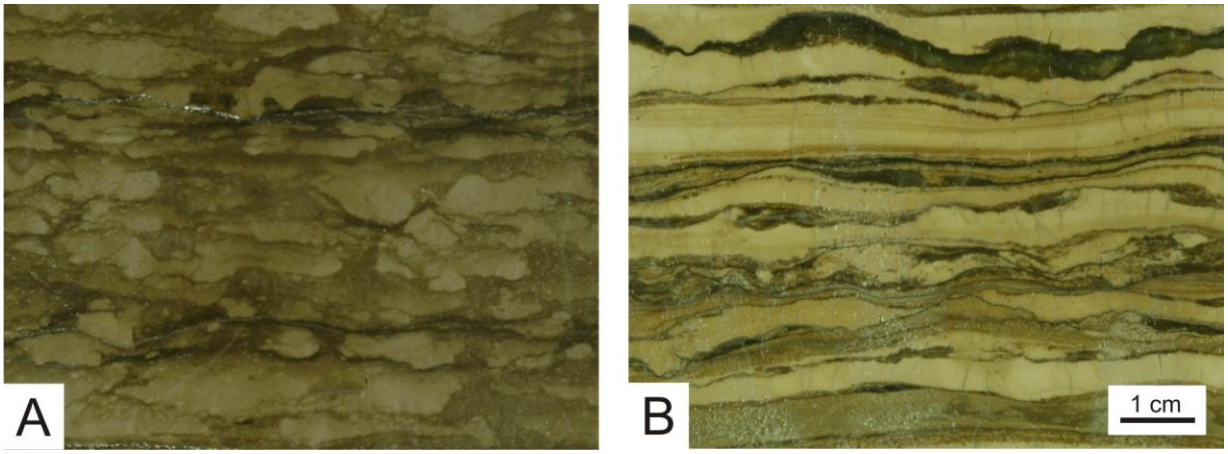

Fig.9. Vertically oriented slab core photographs of soft-sediment deformation. Scale bar same for both. A) Laminae highly disrupted into loop bedding of boudin-like nodules. Basal Lake Alma Member, 15-28-12-2W2, 1935.3 m. B) Slightly disrupted laminae smeared into lenses and loop bedding. Lower Lake Alma Member 05-15-10-02W2, 2324 m

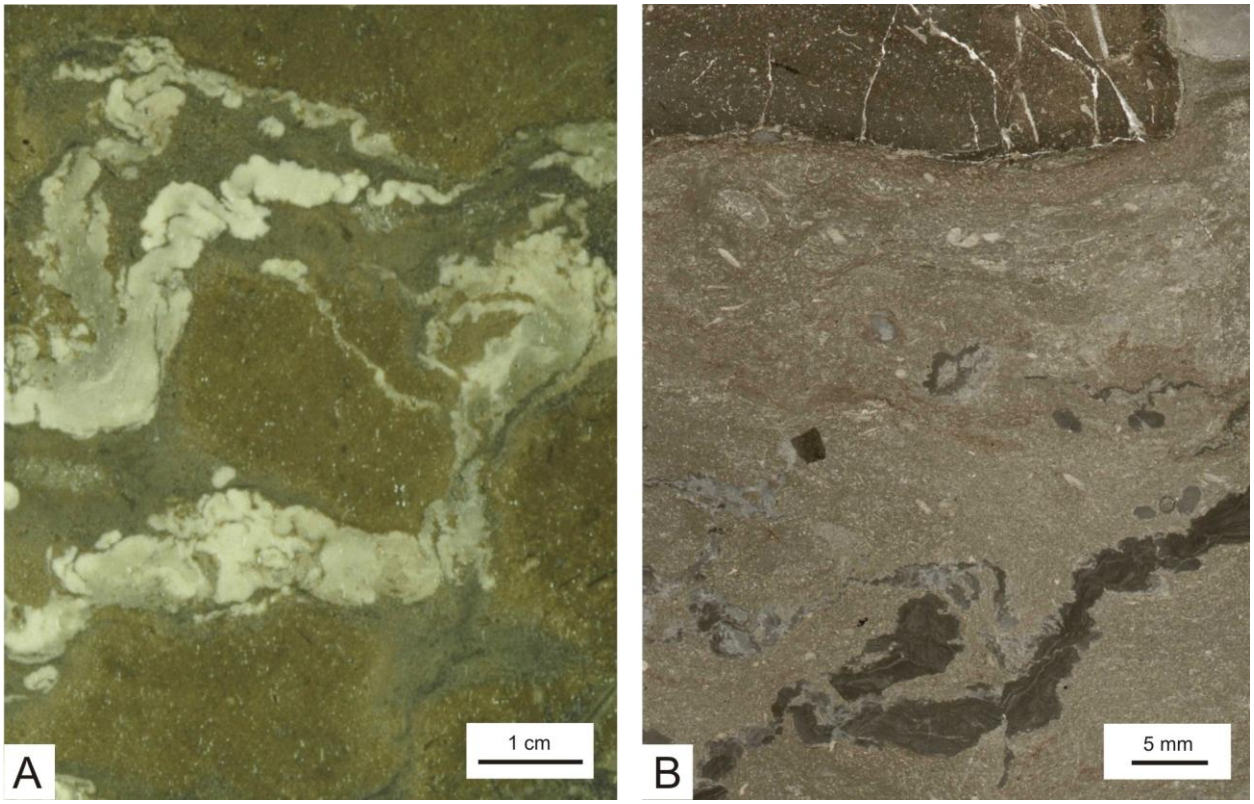

Fig.10. Vertically oriented core (A) and thin section photomicrograph (B) of molar-tooth structure in laminated dolomudstone. Basal Coronach Member. A) Squashed, folded and tilted dikelet. 03-06-06-06W2, 2561 m. B) Tilted and detached, micrite- and microspar-filled dikelet. 14-26-06-11W2, 2563 m.

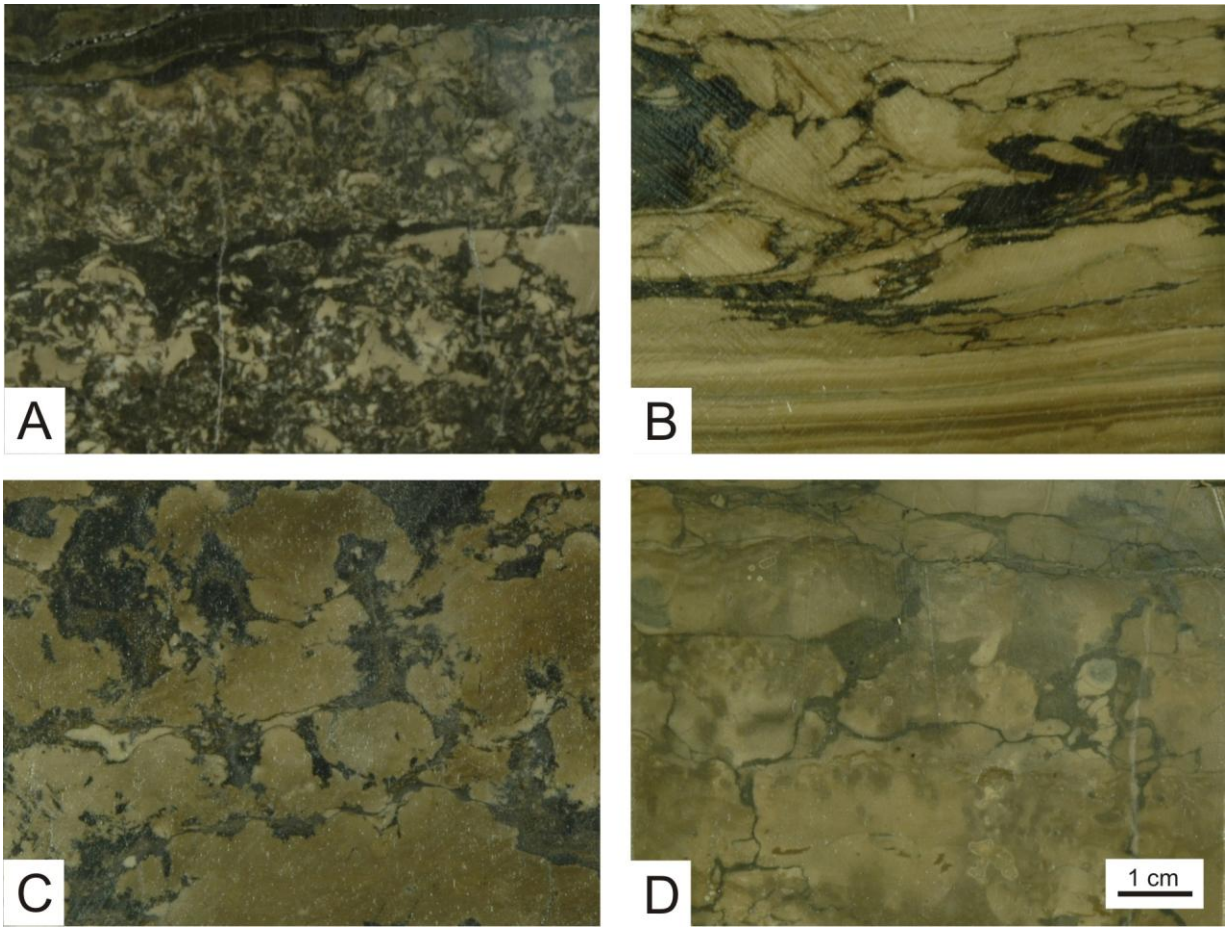

Fig.11. Vertically oriented slabbed cores with quasi-brittle deformation in dolomudstone; scale bar same for all. A) Dolomudstone laminae highly deformed into pseudo-breccia. Lower Coronach Member, 14-26-06-11W2, 2563.5m. B) Disrupted and brecciated lamina. Upper Lake Alma Member, 16-20-08-10W2, 2428m. C) Highly disrupted and pseudo-brecciated massive dolomudstone. Upper Lake Alma Member, 07-16-06-11W2, 2589m. D) Dislocated and pseudo-brecciated dolomudstone. Lower Lake Alma Member, 15-28-12-2W2, 1939 m.

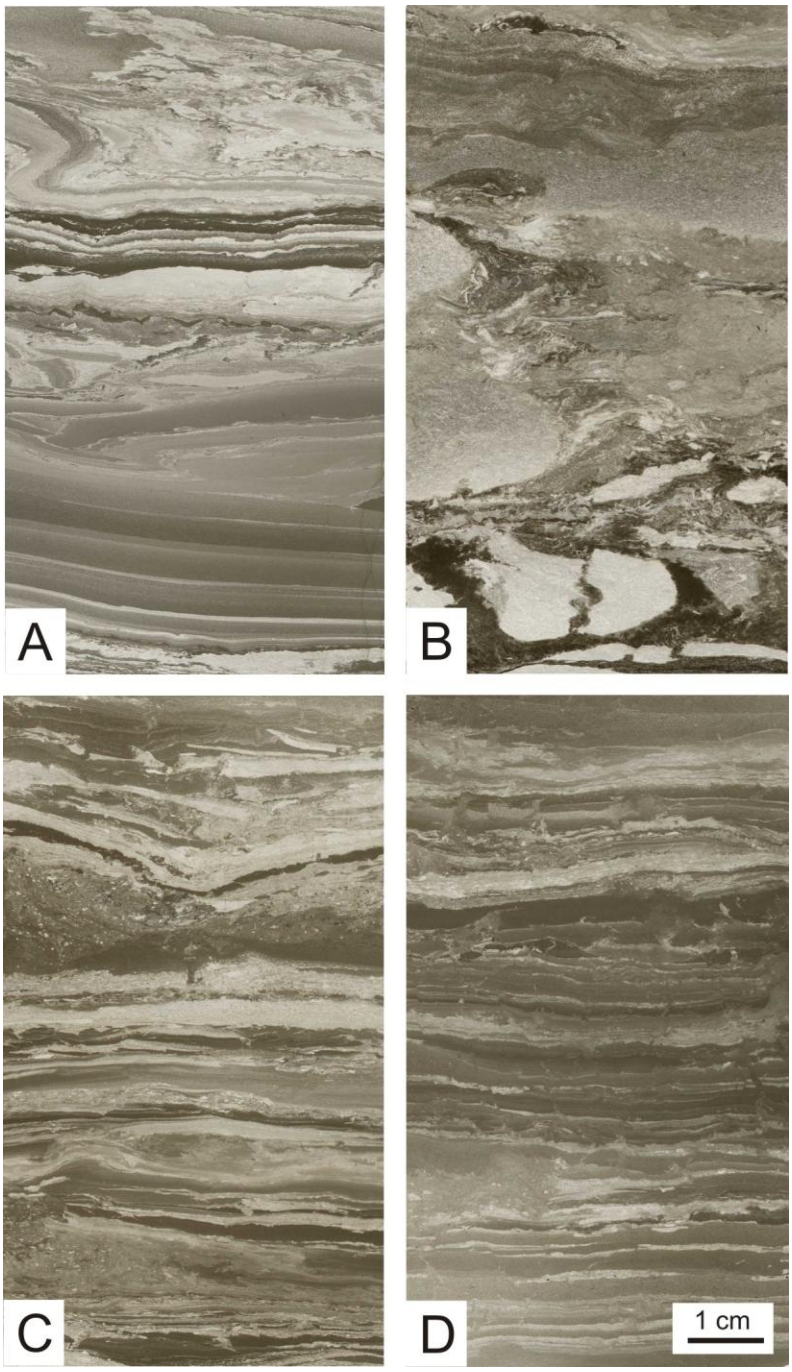

Fig.12. Vertically oriented thin section photomicrographs of soft-sediment and quasi-brittle deformation and brittle failure in laminated dolomudstone. Scale bar same for all. A) Laterally folded laminae and micrite-filled dikelets (top) with disrupted and buckled detached laminae (center-left). Upper Lake Alma Member, 11-17-03-21W2, 2805.3 m. B) Folded laminae (top)

with mud squeezing into undeformed plane thick laminae and mud-filled crack in anhydrite replacement nodule (bottom). Upper Lake Alma Member, 6-18-6-10W2, 2634 m. C) Disrupted and detached laminae, separated by injected sediment; shingled laminae (top) showing weak loop bedding and micro-folding, Basal Coronach Member, 01-14-01-17W2, 3073.6 m. D) Disrupted and detached laminae separated by squeezing short mud dikelets which is moderately disrupted by microfolding (top). Basal Coronach Member, 15-09-02-14W2, 3047.7 m.

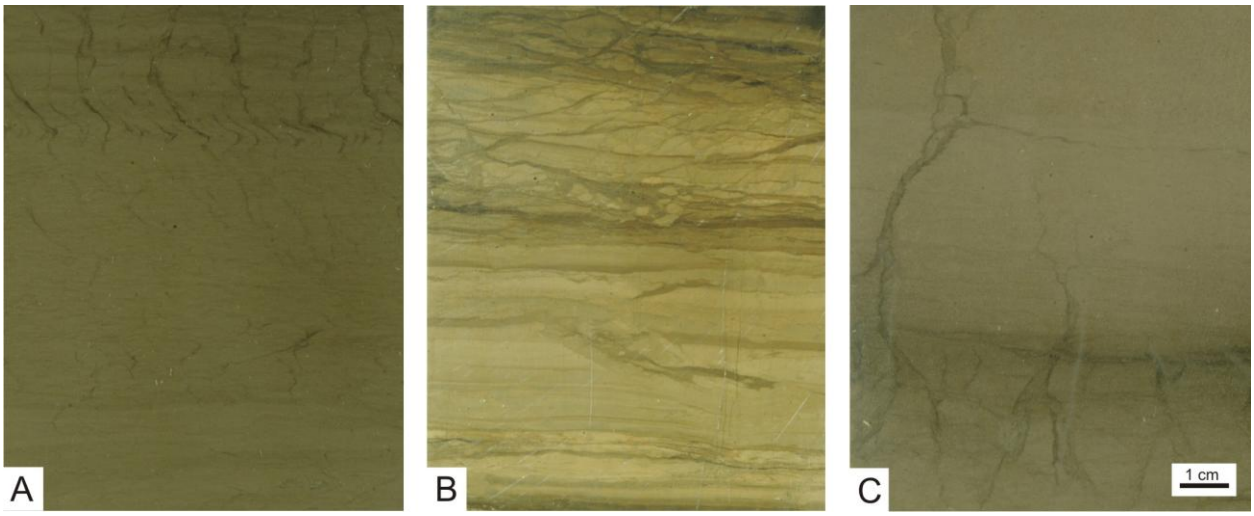

Fig.13. Vertically oriented slabbed cores of quasi-brittle deformation in laminated and massive dolomudstone; scale bar same for all. A) En échelon shear veins in dolomudstone, from Upper Coronach Member 15-08-05-07W2, 2640 m. B) Obliquely oriented en échelon shear veins with pseudo-intraclasts and thrust-like microfaults. Lower Coronach Member, 11-14-07-10W2, 2495m. C) Branching shear veins from Lower Lake Alma Member, 10-25-1-15W2, 3135.7 m.

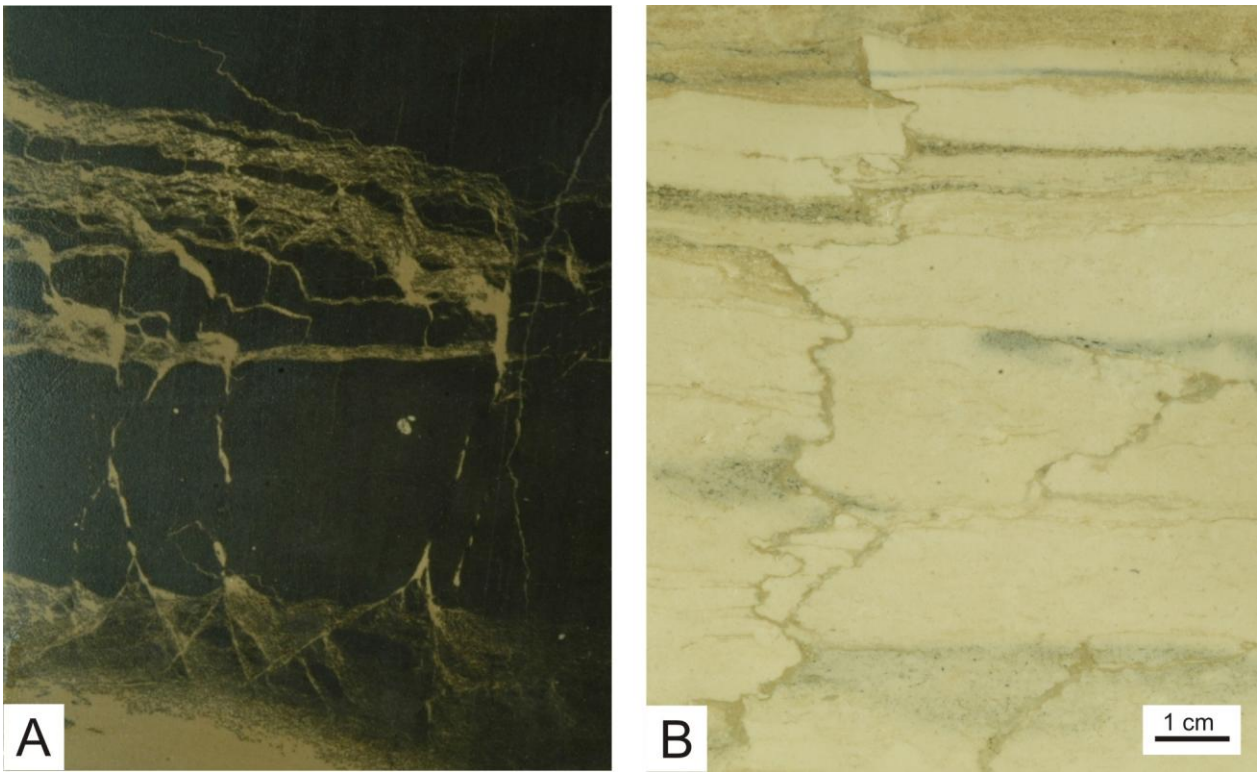

Fig.14. Vertically oriented slabbed cores of laminated dolomudstone sharing brittle failure; scale bar same for all. A) Vertical to oblique mudstone-filled vein arrays, in bitumen shaped impregnated dolomudstone. Lower Lake Alma Member, 08-16-02-14W2, 3032m. B) Zigzagging mudstone-filled microcracks. Lower Lake Alma Member, 05-15-10-02 W2, 2326 m.

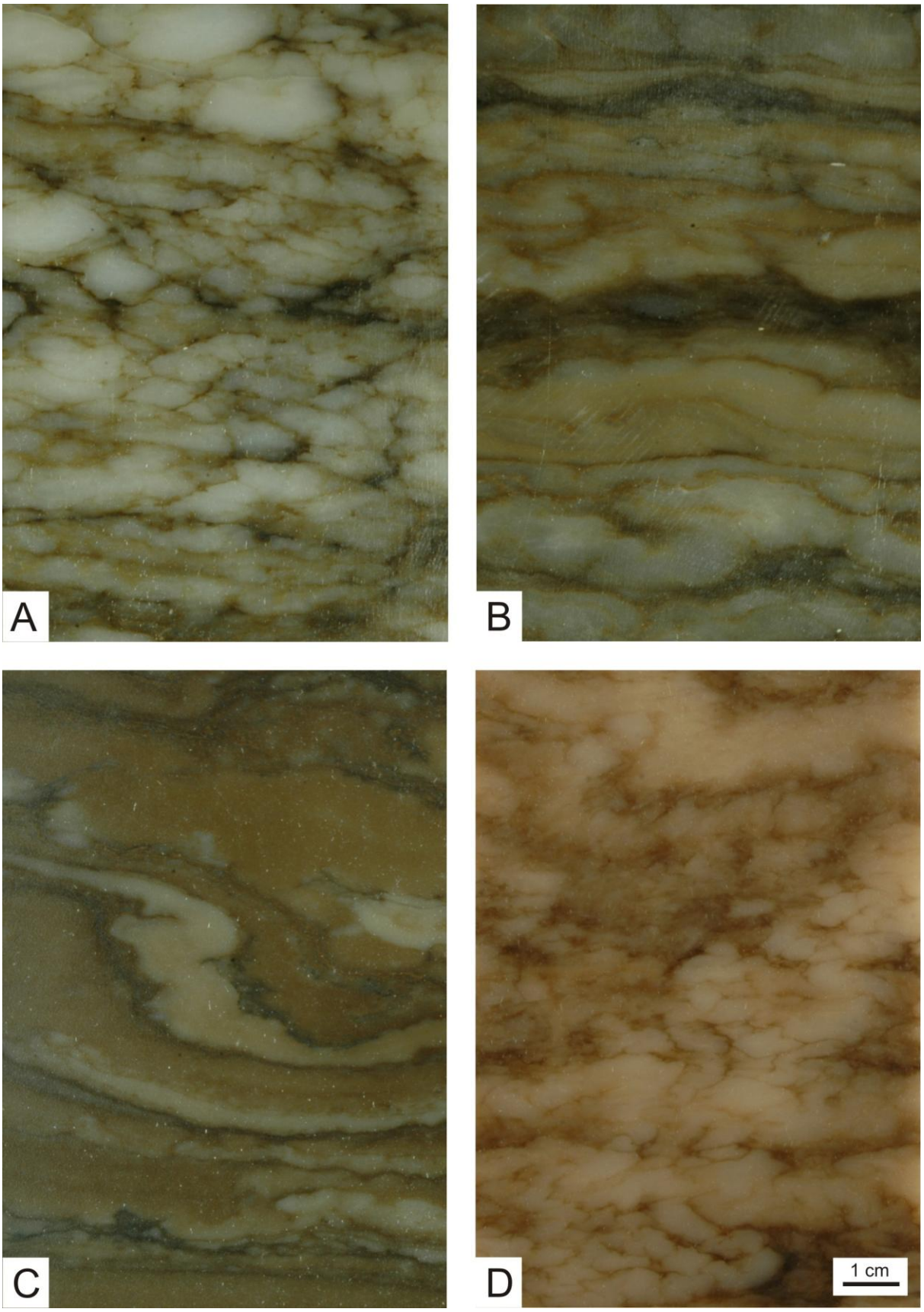
A
B
C
D
1 cm

Fig.15.Vertically oriented slabbed core and thin section photomicrographs of soft-sediment deformation in anhydrite; scale bar same for all. A) Undeformed nodular anhydrite in Upper Lake Alma Member, 15-04-07-10W2, 2540 m. B) Undeformed laminated to nodular anhydrite Upper Lake Alma Member, 14-26-06-11W2, 2564.5 m. C) Microfolding of lamniae at the center and disruption into irregular lenses and nodules Lower Lake Alma Member, 02-08-03-14W2, 2928 m. D) Obliquely folded anhydrite cross-cutting nodular anhydrite, Upper Lake Alma Member 15-09-02-14W2, 3047 m.

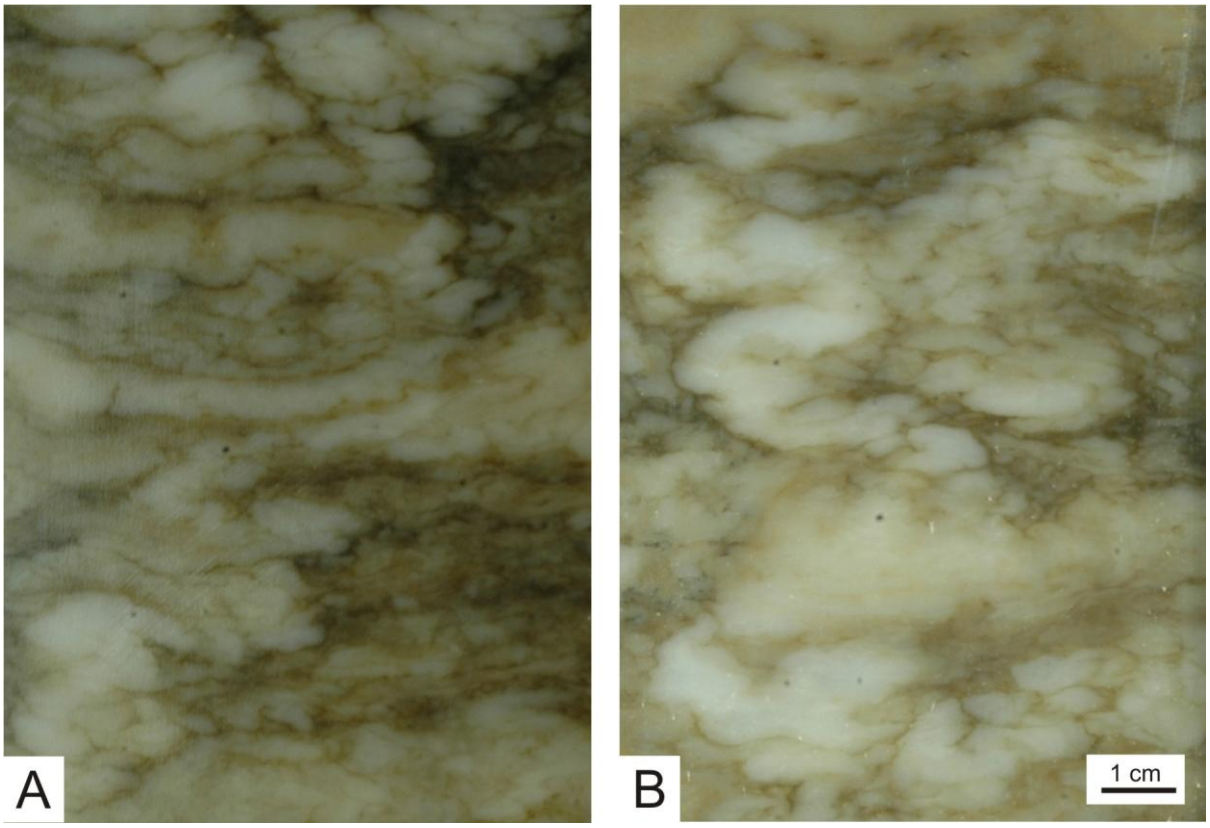

Fig.16.Vertically oriented slabbed cores of anhydrite soft-sediment deformation; scale bar same for all. A) Three obliquely injected dikelets two at the top and one at the bottom and at least two to three smaller squashed dikelets (center) separated by two moderately folded nodular

anhydrite. Upper Lake Alma Member, 08-16-02-14W2, 3028.5 m. B) Two vertical dikelets in between highly disrupted nodular anhydrite. Upper Lake Alma Member. 12-02-07-11W2, 2560.5 m.

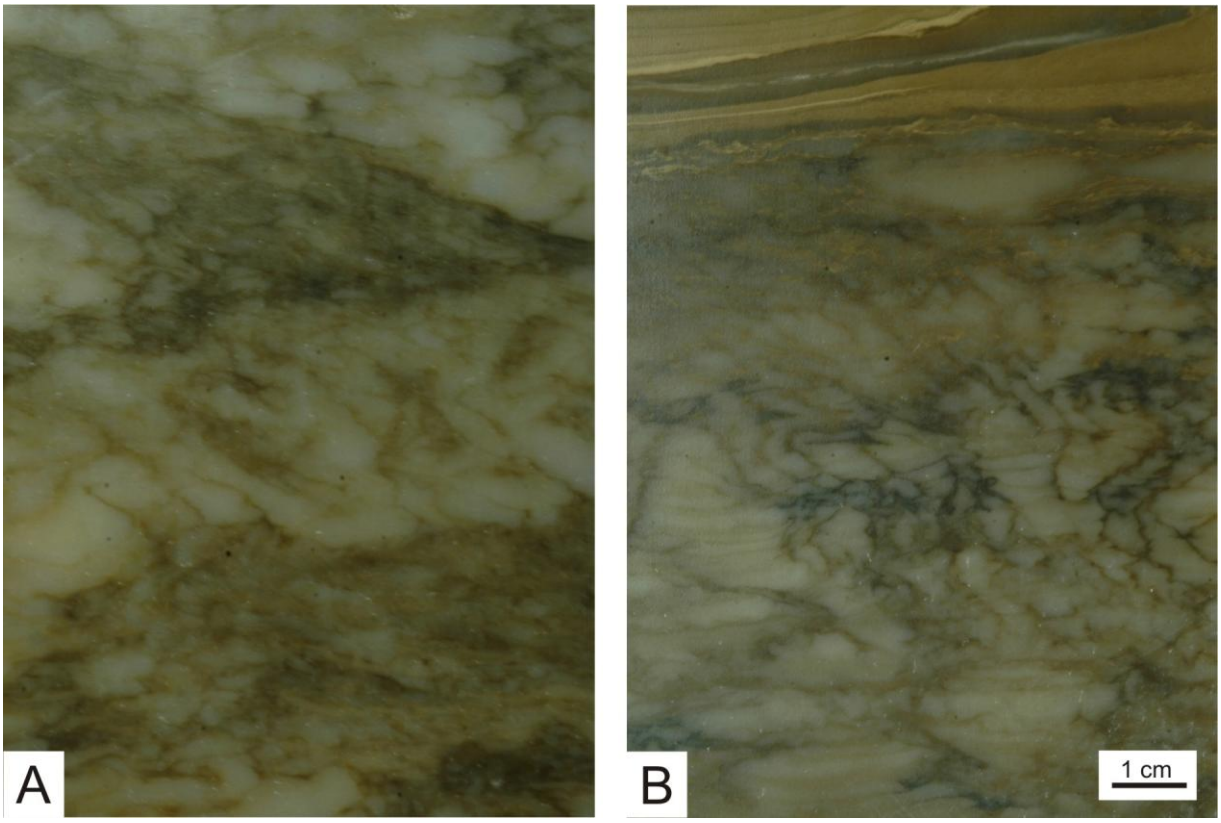

Fig.17.Vertically oriented slabbed cores of anhydrite quasi-brittle deformation; scale bar same for all. A) Obliquely oriented anhydrite that has been folded in between laterally pseudo-brecciated anhydrite. Upper Lake Alma Member, 16-20-08-10W2, 2427.5 m. B) Vertical array of disrupted and squashed irregular boundins. Upper Lake Alma Member, 07-16-06-11W2, 2594.2 m.

DISTRIBUTION OF SEISMITES

Stratigraphic Distribution

Horizons of deformation up to 20 cm thick are taken here as individual seismites presumed to record single earthquake events (of sufficient magnitude, i.e. greater than MM ≥V). This is because no horizons show clear evidence of having been deformed twice, even though theoretically this would be expected because of earthquake clustering and because the record of multiple events is present in other kinds of limestones (Pratt, 1998b, 1999, 2001a, 2001b). This lack of evidence can be ascribed to rapid stiffening of the sediment with, and subsequent to, deformation, such that later events had no appreciable effect.

The stratigraphic distribution of seismites in the Herald Formation is sporadic and variable from well to well (Figures. 18–21). Some wells include up to a dozen seismites while others show only up to one or two deformed horizons. None were observed in the burrowed wackestone–packstone interval in the lower Coronach Member, even though there is some variation in thickness of this interval which suggests differential subsidence. This can be explained in one or more of three ways: (1) during that time there were no strong earthquakes (although there may have been weak ones); (2) there were strong events but the rheology of the bioclastic muddy sediment was such that deformation features did not form; or (3) deformation features did form but were erased by bioturbation.

By contrast, seismites are common in the Lake Alma and upper Coronach members in almost all wells. Dolomudstones exhibit approximately three times more horizons of soft-sediment deformation than those with quasi-brittle and brittle failure (Figures 22 and 23). In cases of quasi-brittle and brittle failure of mudstone laminae, neighbouring sediment flowed around these features, indicating close proximity of contrasting properties. The likely explanation for the predominance of plastic behaviour is relatively rapid stiffening of the lime mud and overall rarity of earthquakes of sufficient magnitude able to disrupt it.

Virtually all the seismites in the anhydrite units of the upper Lake Alma and upper Coronach members record soft-sediment deformation, with a few rare examples of quasi-brittle aspect, which generated the enterolithic aspect of these units. In addition, there are common examples of evaporite injection between nodules and folded laminae. This must have involved mobilization of granular gypsum which took place before transformation from gypsum to anhydrite.

Lime mud injection into concomitantly formed shrinkage cracks, identical to the process inferred for the formation of molar-tooth structure which is common in Proterozoic carbonates (Pratt, 1998b, 2001a, in press), is recorded in wackestones near the base of the lower Coronach Member in several wells. These vein-like features indicate that at only at this horizon was granular lime mud locally able to be segregated from the bioclastic sediment during liquefaction.

Geographic Distribution

Governing the geographic extent of seismites is a combination of the location of the earthquake epicentre, the magnitude of the event, and the lateral persistence of the appropriate sediment rheologies conducive to deformation. Correlation of deformed horizons shows that some appear to be geographically widespread while others are more local. Seismites at the base of the Coronach Member occur over the whole region, suggesting laterally extensive susceptible sediment combined with earthquake events of great magnitude, or possibly concurrent movement of more than one lineament.

The summation of deformation frequency is interpreted to record relative tectonic activity of nearby faults, as expressed by earthquakes of sufficient magnitude (Tables 2, 3, Figures 24 and 25). Wells with a large number of seismites are taken to indicate moderate to high activity, while those with few seismites argue for comparative quiescence. The fairly close geographic proximity of the wells to fault systems thought to have been active because of differential subsidence (Nimegeers and Haidl, 2004) suggests that, because both these features were so close to each other, it may not be possible to differentiate between movements of the Brockton–Froid lineament zone and the Cedoux–Midale trend. However, in cross-section C-C^{1}, the lower frequency of seismites in the west, by contrast to the increasing number towards and over these two features, may suggest an absence of an active fault in the south-central area.

For the sake of discussion, based on the distribution of wells we subdivide the area of study into five quadrants, each comprising a block of four ranges. Seismites in quadrants Q1 and

Q2 show a similar frequency and distribution as those in Q3 and Q4, where active basement faulting has been previously thought to have occurred (Figure 26). This argues for a tectonic element in the former area. This may be an extension of another SW–NE-trending lineament, perhaps contiguous with one recognized in north-central Montana by Potter and Onge (1991; Figure 26), or possibly a SE–NW-trending feature extending into the Hummingbird Trough which is the area of Prairie Evaporite dissolution, as postulated by Kreis and Kent (2002). Further observations are needed to be more certain.

The relative rarity of seismites in the north-central portion of the study area suggests that this area (Q5) was not near to an active structural feature and was only affected by the strongest events originating to the south. Although not based on as much well control, both the eastern and western parts of the study area were also rarely affected by earthquakes, similarly indicating an absence of active tectonic elements.

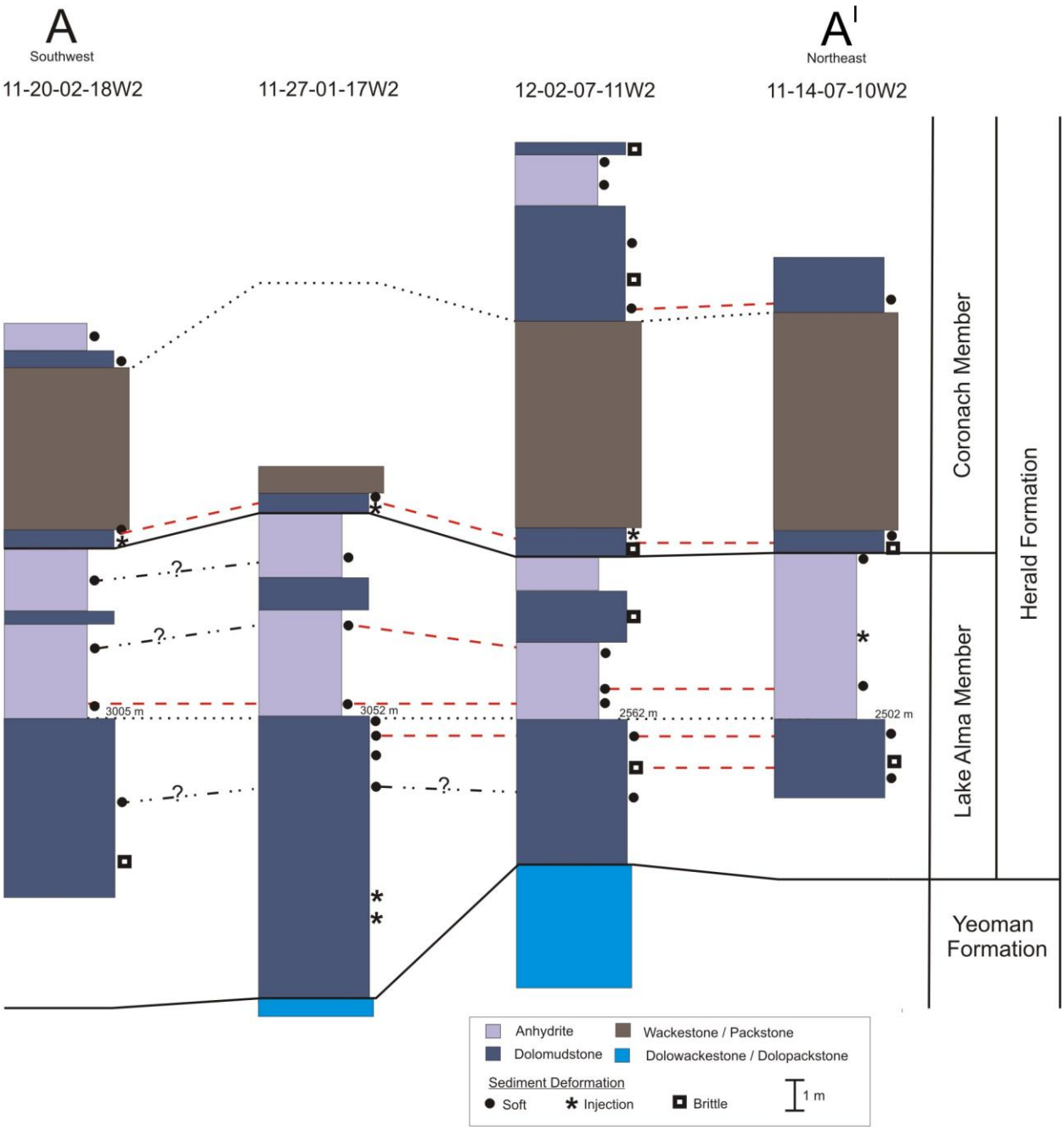

Fig.18. SW–NE cross-section correlating selected wells showing the stratigraphic occurrence of seismites in the Lake Alma and Coronach members located west of the Brockton−Froid lineament zone and southwest of, and over, the Cedoux−Midale trend. Upper solid black line shows correlation of the contact between the two members; lower solid black line defines contact between the Yeoman Formation and Lake Alma Member. Dotted line is datum at the base of the

anhydrite comprising the upper Lake Alma Member. Dashed red lines show individual seismites that appear to be laterally continuous. Possible correlations are represented by dashed lines.

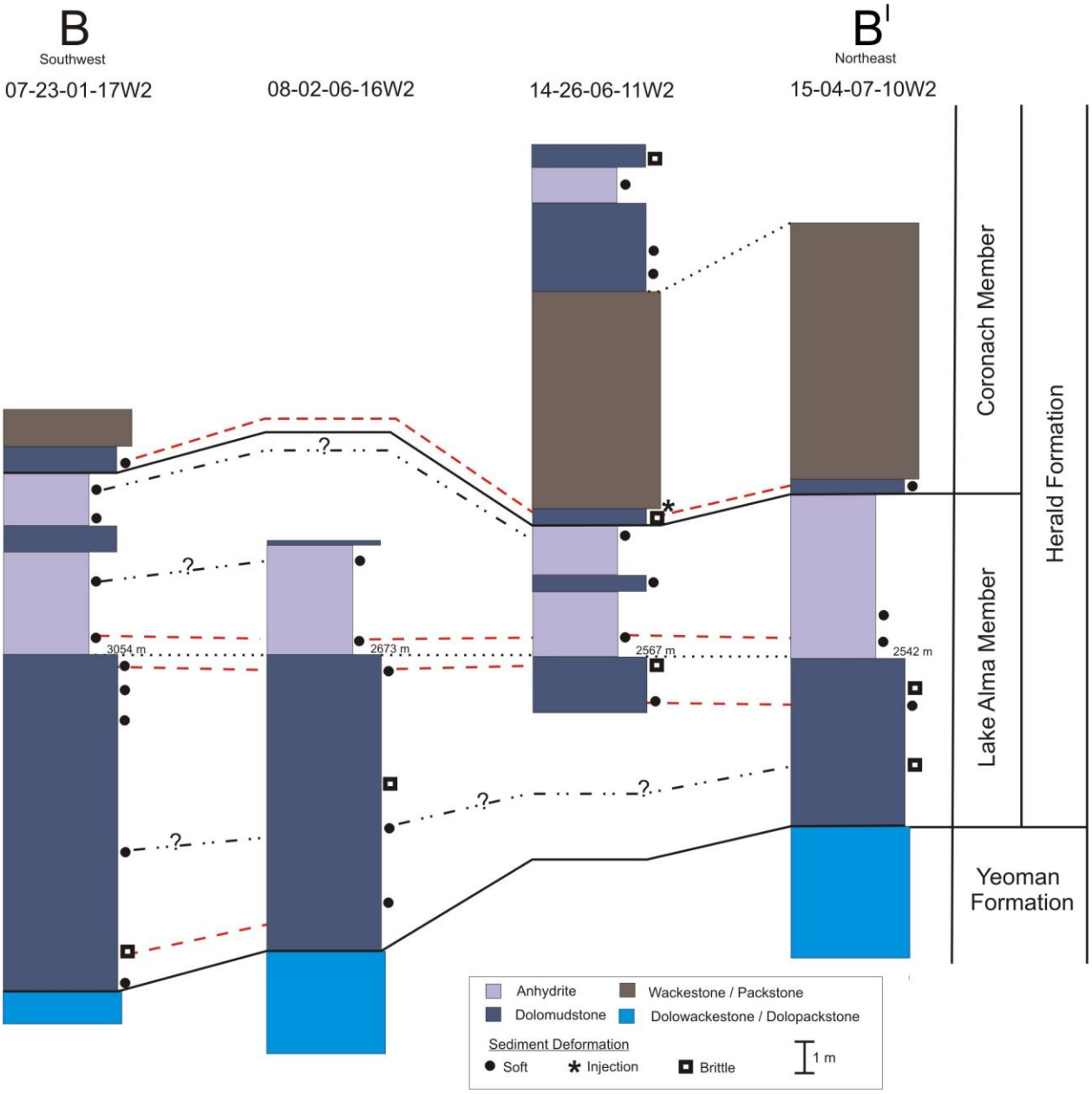

Fig.19. SW–NE cross-section located west of the Brockton−Froid lineament zone and west, southwest of, and over, the Cedoux−Midale trend.

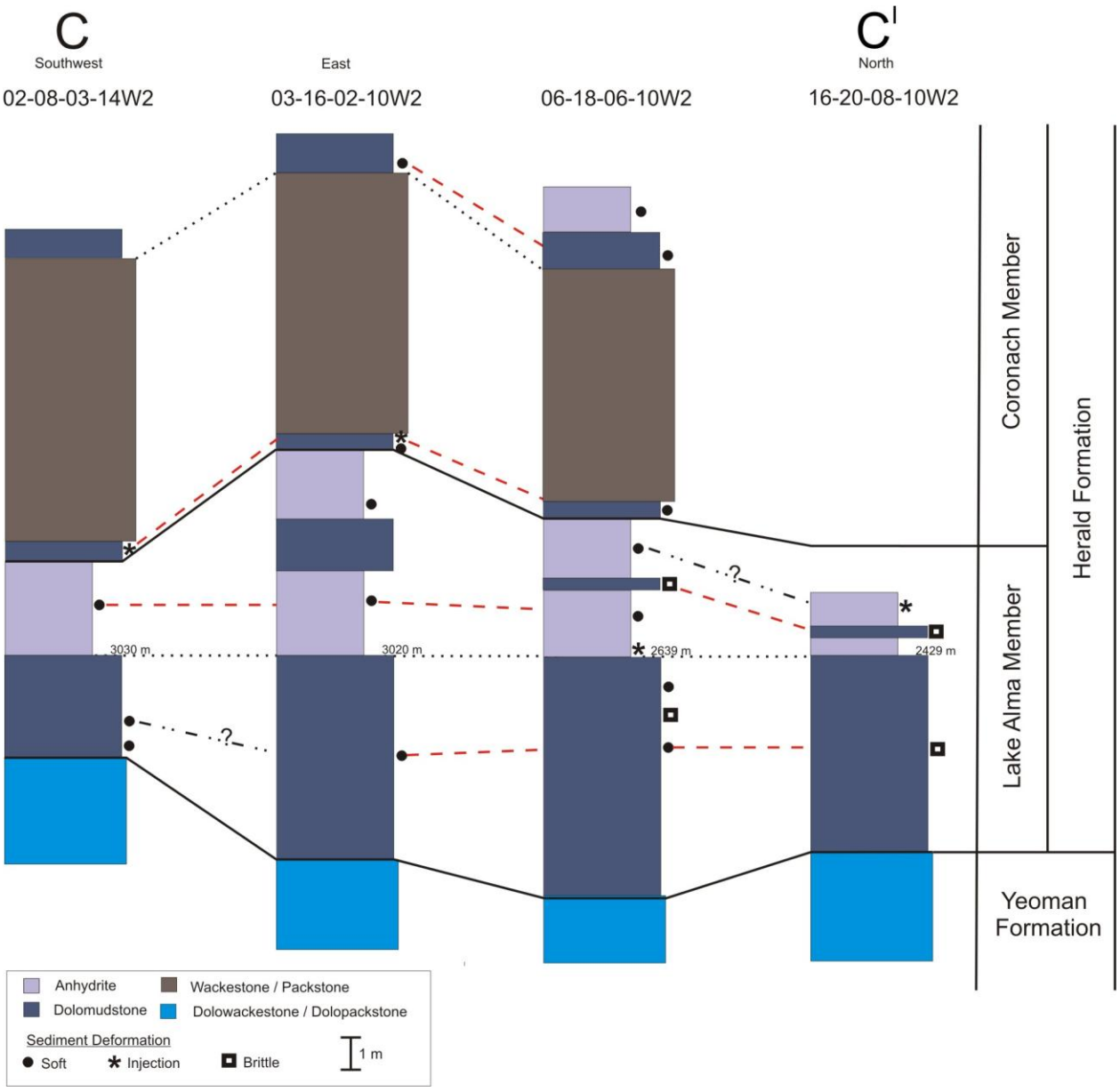

Fig.20. SW–E–N cross-section located west of the Brockton−Froid lineament zone and over the Cedoux−Midale trend.

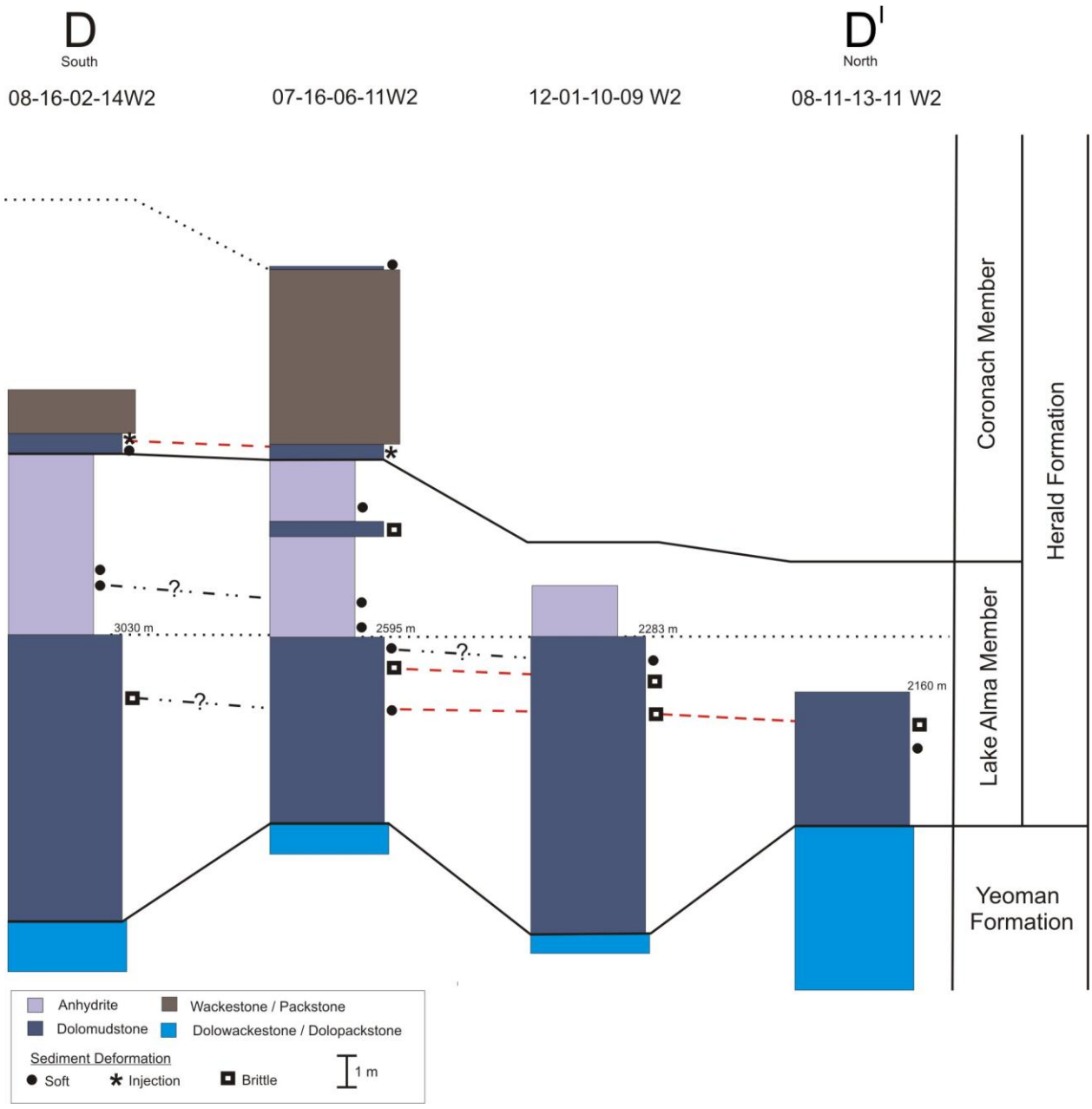

Fig.21. S–N cross-section located west of the Brockton−Froid lineament zone, and over, the Cedoux−Midale trend and Montmartre−Weir Hill trend.

Quadrant	Well	Stratigraphic Unit	Deformation Type		Seismite Frequency	Tectonic Activity
			Soft	Brittle		
Q1	01-14-01-17W2	Lower Lake Alma Member	√	√	4	Moderate to high
	11-27-01-17 W2		√		6	
	13-23-01-17W2		√	√	3	
	07-23-01-17W2		√	√	6	
	11-20-02-18W2		√	√	2	
Q2	08-16-02-14W2	Lower Lake Alma Member		√	1	Moderate
	02-08-03-14W2		√		2	
	10-25-01-15W2		√	√	4	
	14-15-03-15W2		√	√	6	
	15-09-02-14 W2		√	√	2	
Q3	12-02-07-11W2	Lower Lake Alma Member	√	√	3	Moderate
	06-18-06-10 W2		√	√	3	
	11-14-07-10 W2		√	√	3	
	07-16-06-11 W2		√	√	3	
	12-33-06-11W2		√	√	3	
Q4	03-06-06-06W2	Lower Lake Alma Member	√		2	Moderate
	09-29-06-06W2		√		3	
	14-06-06-06W2		√	√	4	
	15-30-06-06W2		√	√	3	
	15-08-05-07W2		√	√	3	

Table.1. Distribution relationship between sediment deformation type, frequency and tectonic activity in wells from Lower Lake Alma Member. Quadrants (Q1, Q2, Q3 and Q4) show more or less similar fault-related tectonic activity. Values are not given for Q5 due to the lack of core.

Quadrant	Well	Stratigraphic Unit	Deformation Type		Seismite Frequency	Tectonic Activity
			Soft	Brittle		
Q1	01-14-01-17W2	Upper Lake Alma Member	√		4	Moderate
	11-27-01-17 W2		√		3	
	13-23-01-17W2		√		3	
	07-23-01-17W2		√		4	
	11-20-02-18W2		√		3	
Q2	08-16-02-14W2	Upper Lake Alma Member	√		2	Low
	02-08-03-14W2		√		1	
	10-25-01-15W2		√		1	
	14-15-03-15W2		√		1	
	15-09-02-14 W2		√	√	3	
Q3	12-02-07-11W2	Upper Lake Alma Member	√	√	4	Moderate
	06-18-06-10 W2		√	√	4	
	11-14-07-10 W2		√		3	
	07-16-06-11 W2		√	√	4	
	12-33-06-11W2		√		2	
Q4	03-06-06-06W2	Upper Lake Alma Member	√		1	Low
	09-29-06-06W2		√		0	
	14-06-06-06W2		√		1	
	15-30-06-06W2		√		1	
	15-08-05-07W2		√		2	

Table.2. Distribution relationship between sediment deformation type, frequency and tectonic activity in wells from upper Lake Alma Member. Quadrants (Q1, Q2, Q3 and Q4) show at least two discrete areas of different tectonic activity. Values are not given for Q5 due to the lack of core.

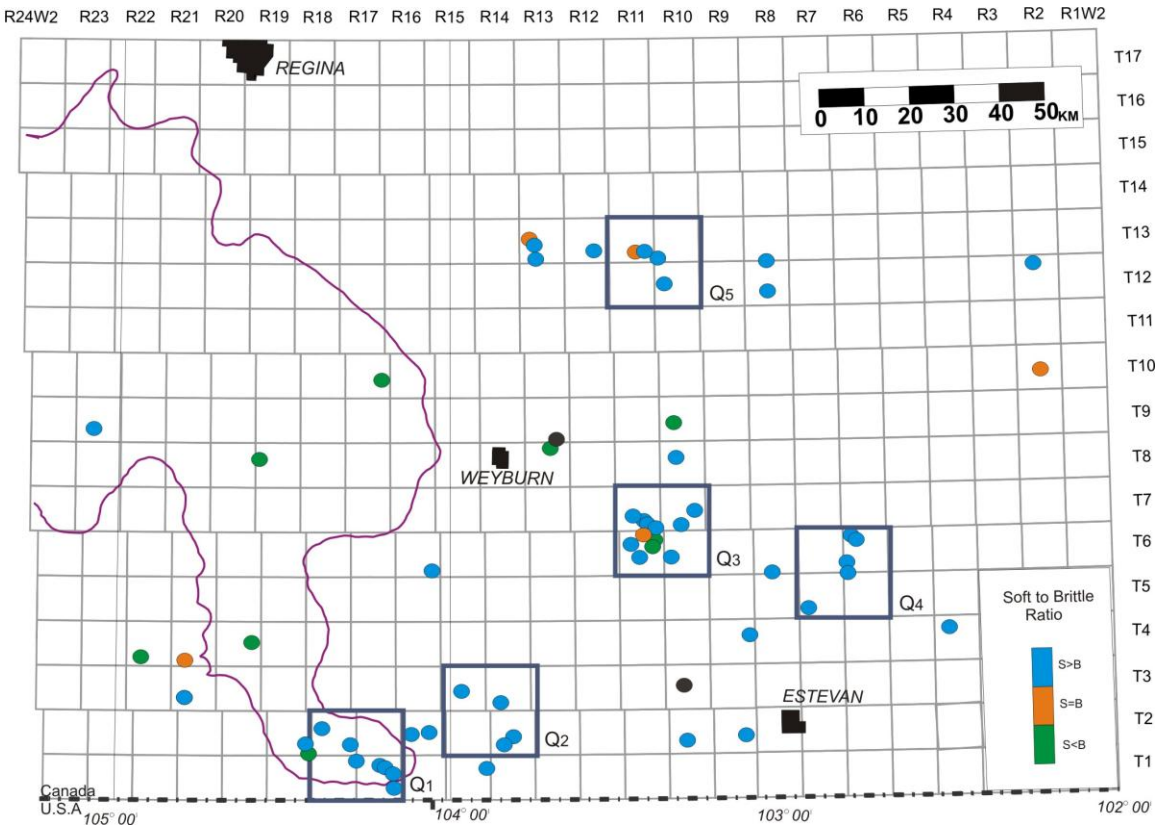

Fig.22. Map showing the distribution of different ratios of soft-sediment deformation to brittle failure traced from wells in the investigated area. Soft-sediment deformation dominates over brittle failure.

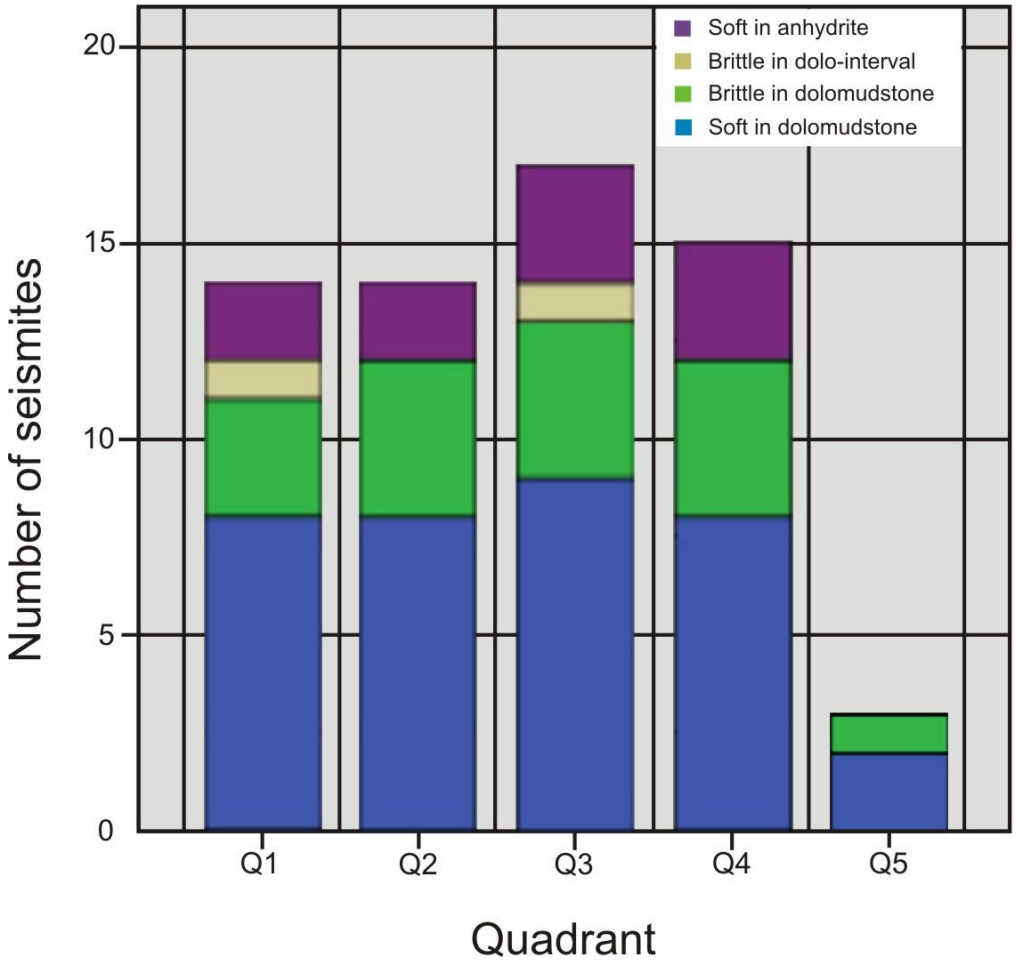

Fig.23. Bar graph showing the number of seismite horizons of soft-sediment deformation and brittle failure in dolomudstone and anhydrite from different geographic regions Q1, Q2, Q3, Q4 and Q5. Seismite frequency number in Q5 is lower than the other quadrants due to the lack of core section of upper Lake Alma and Lower Coronach members.

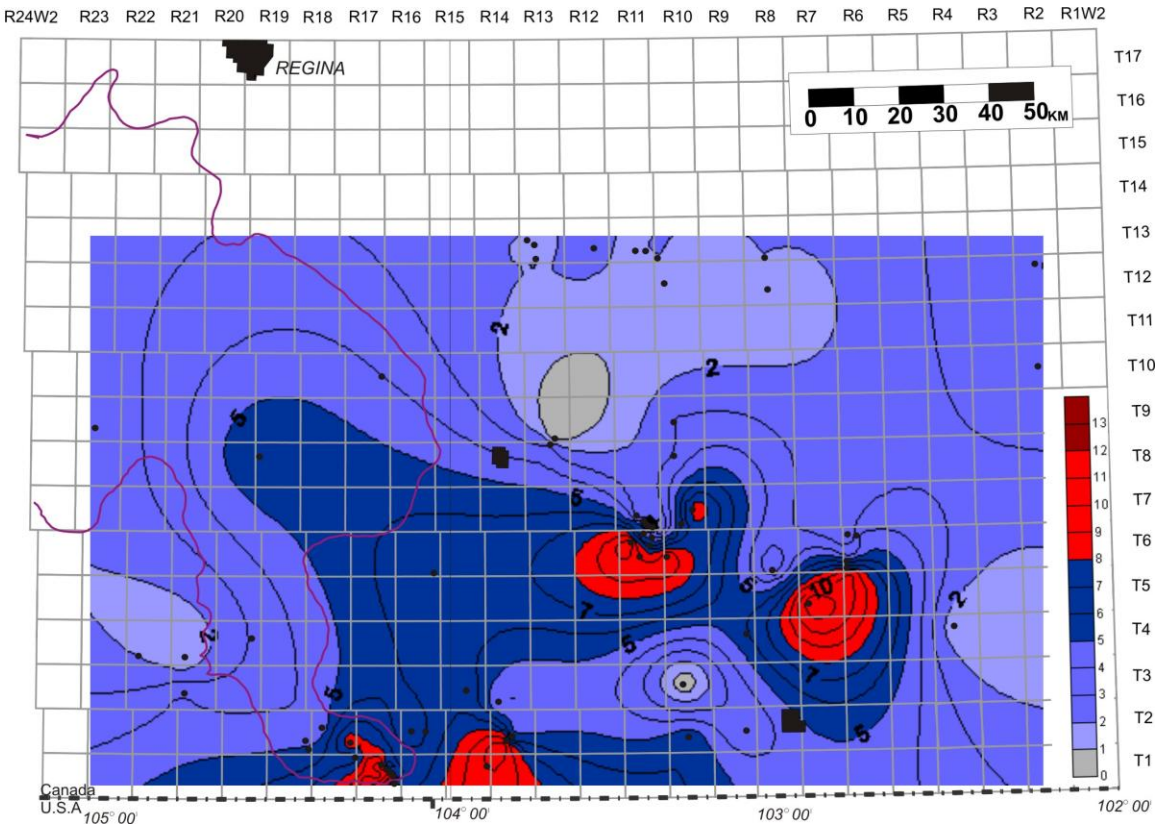

Fig. 24. Isopleth map showing the centres of interpreted high seismicity for the Lake Alma and both lower and upper Coronach members. Contour interval 1 of soft-sediment deformation and brittle failure frequency.

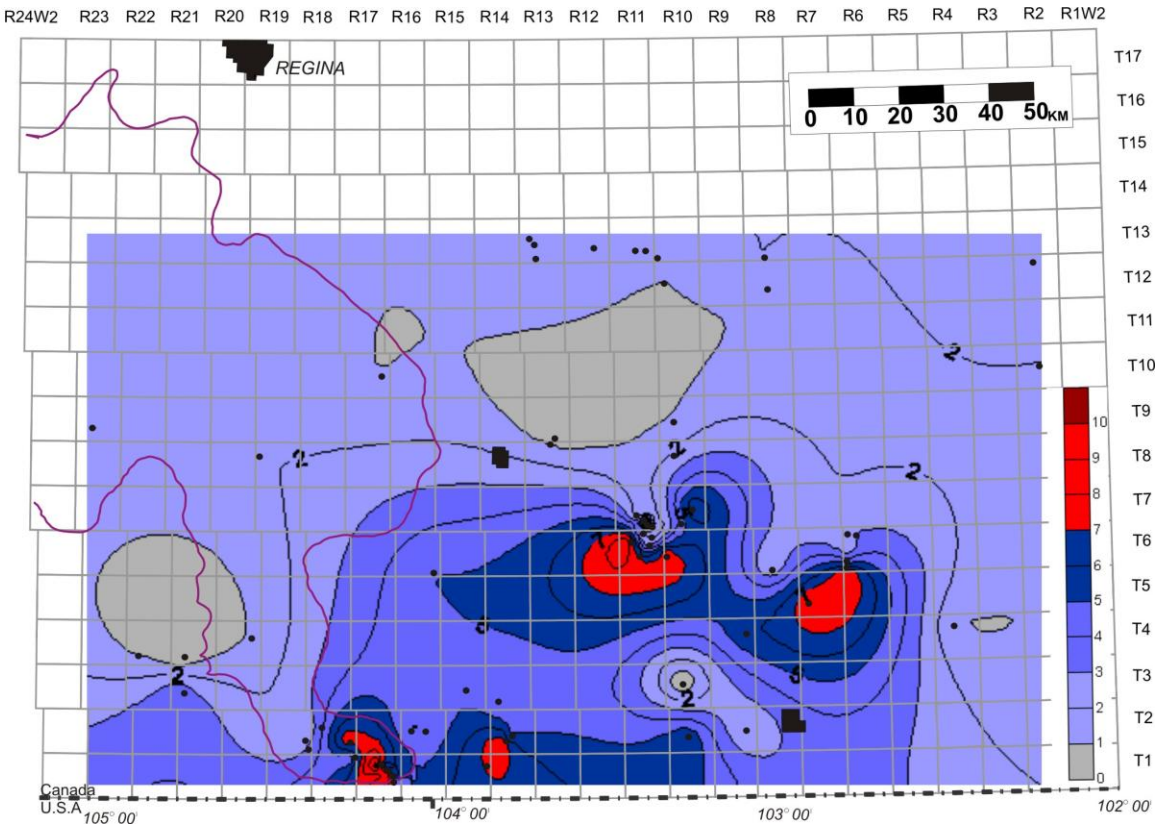

Fig.25 Isopleth map showing centres of high seismicty for the Lake Alma and lower Coronach members. Contour interval 1 of soft-sediment deformation frequency.

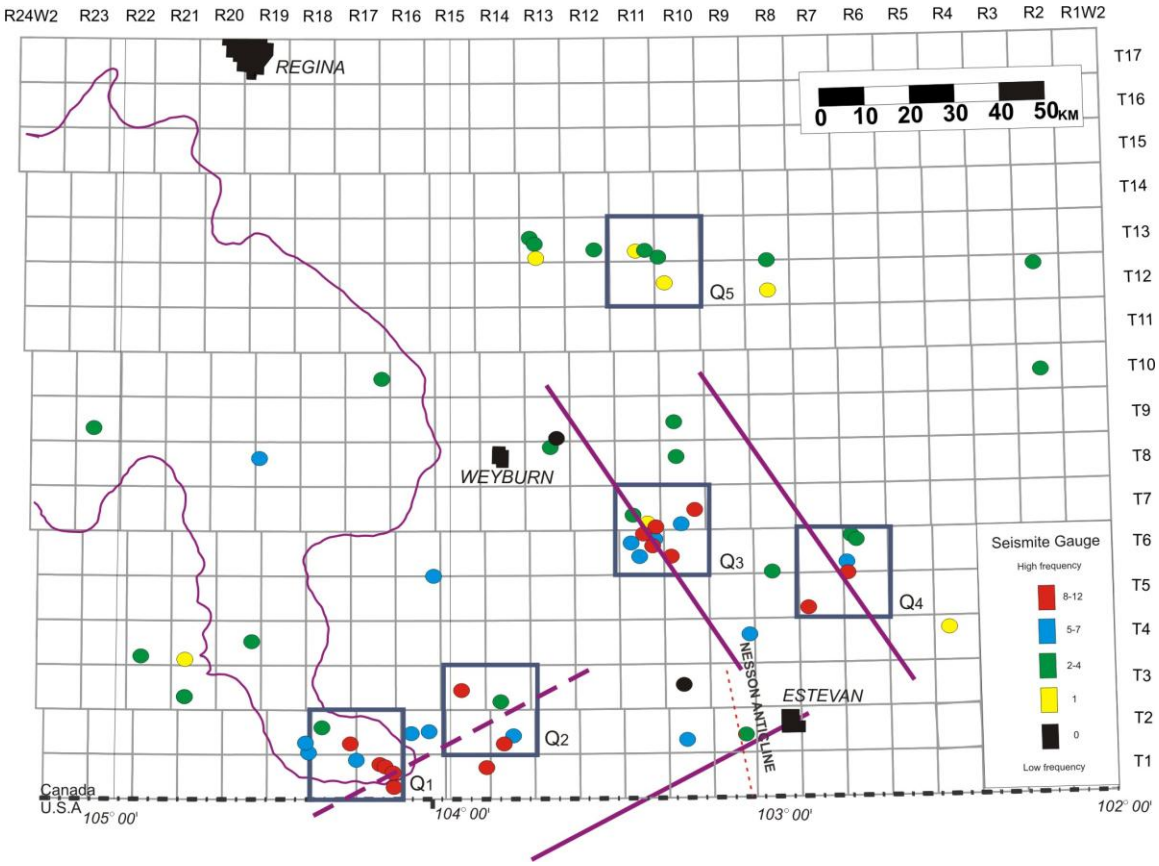

Fig.26. Geographical distribution of levels of seismite frequency in the Herald Formation in five quadrants consisting of four sections each, southeastern Saskatchewan. Seismite frequency is interpreted to equate to seismicity of the nearby texture element (lineaments) shown by purple lines (based on Figure 3; Nimegeers and Haidl, 2004). Dashed lineament is hypothetical on the basis of seismite frequency in quadrants 1 and 2; and shown as parallel to Brockton–Froid lineament.

CONCLUSIONS

Late Ordovician sediments comprising Red River strata in southeastern Saskatchewan contain syn-depositional deformation features referred to as seismites. Horizons of these seismites are present in low-energy units of the Herald Formation that were taphonomically conducive to preservation. The underlying basement tectonic configuration consists of a series of lineaments that have an orthogonal alignment oriented NW−SE and NE–SW. Distinct variation in the thickness of the Herald Formation in this part of the Williston Basin was due to differential subsidence probably caused by far-field stresses likely originating from the Taconic orogeny in eastern Laurentia.

The variety of seismites observed in laminated and massive dolomudstone and laminated to nodular anhydrite includes convolute bedding, micro-folds, loop bedding, vein arrays, cracks, micro-faults, breccias, and dikelets from sediment injection. This range of features records soft-sediment and quasi-brittle deformation to brittle failure caused by earthquake-induced ground motion, that is, shaking of the sea bottom and shallow-buried sediments of varying rheology.

Correlation of seismite horizons observed in cores shows that the basal part of the Coronach Member and the lowermost part of the Lake Alma anhydrite record at least one regionally widespread event, while most other seismites appear to have been more restricted geographically. However, an estimation of seismicity for the region is possible since correlation shows variable frequencies of these localized seismites. Multiple earthquake events in the same vicinity are evidence for repeated movement along discrete basement faults. Geographical

variation suggests that some faults were more active than others, either in terms of frequency of events or the magnitude of the earthquakes they generated.

Ultimately, given the limitations and biases of the database due to the availability of core and the distribution of wells relative to the underlying structural fabric, the summation of seismite frequency in parts of the Herald Formation serves not only as a valid proxy for determining seismicity, but also has the potential to provide a window into understanding the location and timing of movement of basement structural elements in southeastern Saskatchewan. It is possible that one or more of these elements may have hitherto gone unrecognized via conventional geophysical observation. In turn, in regions with less subsurface control or limited outcrop, the presence and distribution of seismites provide valuable clues to the structural and depositional history that have yet to be widely recognized and exploited.

REFERENCES

Allen, J.R.L. 1986. Earthquake magnitude–frequency, epicentral distance, and soft-sediment deformation in sedimentary basins. Sedimentary Geology, v. 46, p. 67–75.

Bergström, S.M., Chen, X., Gutiérrez-Marco, J.C. and Dronov, A. 2009. The new chronostratigraphic classification of the Ordovician System and its relations to major regional series and stages and to δ^{13}C chemostratigraphy. Lethaia, v. 42, p. 97−107.

Brothers, R.J., Kemp, A.E.S. and Maltman, A.J. 1996. Mechanical development of vein structures due to the passage of earthquake waves through poorly consolidated sediments. Tectonophysics, v. 260, p. 227–244.

Calvo, J.P., Rodríguez-Pascua, M., Martín-Velázquez, S., Jiménez, S. and De Vicente, G. 1998. Microdeformation of lacustrine laminite sequences from Late Miocene formations of SE Spain: an interpretation of loop bedding. Sedimentology, v. 45, p. 279−292.

El-Isa, Z.H. and Mustafa, H. 1986. Earthquake deformations in the Lisan deposits and seismotectonic implications. Geophysical Journal, v. 86, p. 413–424.

El Taki, H. and Pratt, B.R. 2009. Synsedimentary deformation in laminated dolostones and evaporites of the Herald Formation (Red River): signature of Late Ordovician tectonic activity in southern Saskatchewan. In: Summary of Investigations 2009, Volume 1, Saskatchewan Geological Survey, Saskatchewan Industry and Resources, Miscellaneous Report 2009- 4.1, Paper A3, p. 10.

Fortuin, A.R. and Dabrio, C.J. 2008. Evidence for Late Messinian seismites, Níjar Basin, south - east Spain. Sedimentology, v. 55, p. 1595−1622.

Fossen, H., Schultz, R.A., Shipton, Z.K. and Mair, K. 2007. Deformation bands in sandstone: a review. Journal of the Geological Society, London, v. 164, p. 755–769.

Greggs, R.G. and Greggs, D.H. 1989. Fault block tectonism in the Devonian subsurface, Western Canada Basin: Journal of Petroleum Geology, v. 12, p. 377−404.

Gerhard, L.C., Anderson, S.B. and Fischer, D.W. 1991. Petroleum geology of the Williston basin. In: Petroleum Geology of Interior Cratonic Basins. M. Leighton, D. Kolata, D. Oltz and J. Eidel (eds.). American Association of Petroleum Geologists, Memoir 51, p. 507–559.

Kahle, C.F. 2002. Seismogenic deformation structures in microbialites and mudstones, Silurian Lockport Dolomite, northwestern Ohio, U.S.A. Journal of Sedimentary Research, v. 72, p. 201−216.

Kendall, A.C. 1976. The Ordovician Carbonate Succession (Bighorn Group) of Southeastern Saskatchewan. Department of Mineral Resources, Saskatchewan Geological Survey, Report 180, 186 pp.

Kent, D.M. 2003. Some thoughts on the formation of calcium sulphate deposits in Paleozoic Rocks of Southern Saskatchewan. In: Summary of Investigations 2003: Saskatchewan Geological Survey, Saskatchewan Industry and Resources, Miscellaneous Report 2003-4.1, Paper A-8.

Kirkland, D.W. 2003. An explanation of the varves of the Castile Evaporites (Upper Permian) Texas and New Mexico, USA. Sedimentology, v. 50, p. 899−920

Kirkland, D.W. and Anderson, R.Y. 1970. Microfolding in the Castile and Todilto evaporites, Texas and New Mexico. Geological Society of America Bulletin, v. 81, p. 3259−3282.

Kreis, L.K. and Kent, D.M. 2000. Basement controls on Red River sedimentation and hydrocarbon production in southeast Saskatchewan. In: Summary of Investigations 2000, Saskatchewan Geological Survey, Saskatchewan Energy and Mines, Miscellaneous Report 2000-4.1, p. 21−42.

Kreis, L.K., Haidl, F.M., Nimegeers, A.R., Ashton, K.E., Maxeiner, R.O. and Coolican J. 2004. Lower Paleozoic map series – Saskatchewan. Saskatchewan Geological Survey, Saskatchewan Industry and Resources, Miscellaneous Report 2004-8.

Lefever, J.A., Lefever, R.D. and Anderson, S.D. 1987. Structural evolution of the central and southern portions of the Nesson anticline, North Dakota. In: Fifth Williston Basin Symposium. C.G. Carlson and J.E. Christopher (eds.). Saskatchewan Geological Society, Special Publication 9, p. 147−156.

Longman, M.W. and Haidl, F.M. 1996. Cyclic deposition and development of porous dolomites in the Upper Ordovician Red River Formation, Williston basin. In: Paleozoic Systems of the Rocky Mountain Region, Rocky Mountain Section. M.W. Longman and M.D. Sonnenfeld (eds.). Society for Sedimentary Geology, p. 29–46.

Maltman, A. 1984. On the term “soft-sediment deformation”. Journal of Structural Geology, v. 6, p. 589−592.

Marco, S. and Agnon, A. 2005. High resolution stratigraphy reveals repeated earthquake faulting in the Masada fault zone, Dead Sea transform: Tectonophysics, v. 408, p. 101−112.

Migowski, C., Agnon, A., Bookman, R., Negendank, J.F.W. and Stein, M. 2004. Recurrence pattern of Holocene earthquakes along the Dead Sea transform revealed by varve-counting and radiocarbon dating of lacustrine sediments. Earth and Planetary Science Letters, p. 301−314.

Montenat, C., Barrier, P., d'Estevou, P.O. and Hibsch, C. 2007. Seismites: an attempt at critical analysis and classification. Sedimentary Geology, v. 196, p. 5−30.

Moretti, M. 2000. Soft-sediment deformation structures interpreted as seismites in middle-late Pleistocene aeolian deposits (Apulian foreland, southern Italy). Sedimentary Geology, v. 135, p. 167–179.

Moretti, M, Peiri, P. and Tropeano, M. 2002. Late Pleistocene soft sediment deformation structures interpreted as seismites in paralic deposits in the city of Bari (Apulian foreland, southern Italy). Geologic Society of America, Special papers 359 p 75–86

Moretti, M. and Sabato, L. 2007. Recognition of trigger mechanisms for soft-sediment deformation in the Pleistocene lacustrine deposits of the Sant Arcangelo Basin (Southern Italy): seismic shock vs. Overloading. Sedimentary Geology, v. 196, p. 31−45.

Nimegeers, A.R. and Haidl, F.M. 2004. Lower Paleozoic anhydrites in southeastern Saskatchewan (Townships 1 to 17, Ranges 1W2 to 24W2). In: Summary of Investigations 2004, Saskatchewan Geological Survey, Saskatchewan Industry and Resources, Miscellaneous Report 2004-4.1, Paper A-4.

Onasch, C.M. and Kahle, C.F. 2002. Seismically induced soft-sediment deformation in some Silurian carbonates, eastern U.S. Midcontinent. In: Ancient Seismites. F.R. Ettensohn, N. Rast and C.E. Brett (eds.). Geological Society of America Bulletin, Special Paper 359, p. 165−176.

Oglesby, C.A. 1987. Distinguishing between depositional and dissolution thinning: Devonian Prairie Formation, Williston Basin, North America. In: Fifth Williston Basin Symposium, Symposium. C.G. Carlson and J.E. Christohper (eds.). Saskatchewan Geological Society, Special Publication 9, p. 47–52.

Ortner, H. 2007. Styles of soft-sediment deformation on top of a growing fold system in the Gosau Group at Muttekopf, Northern Calcareous Alps, Austria: slumping versus tectonic deformation. Sedimentary Geology, v. 196, p. 99−118.

Owen, G. 1987. Deformation processes in unconsolidated sands. In: Deformation of Sediments and Sedimentary Rocks. M.E. Jones and R.M.F. Preston (eds.). Geological Society Special Publication 29, p. 11−24.

Owen, G. 1995. Soft-sediment deformation in upper Proterozoic Torridonian sandstones (Applecross Formation) at Torridon, Northeast Scotland. Journal of Sedimentary Research, v. 65, p. 495−504.

Owen, G. 1996. Experimental soft-sediment deformation: structures formed by the liquefaction of unconsolidated sands and some ancient examples. Sedimentology, v. 43, p. 279−293.

Paz, J.D.S. and Rossetti, D.F. 2005. Linking lacustrine cycles with syn-sedimentary tectonic episodes: an example from the Codo Formation (Late Aptian), northern Brazil. Geological Magazine, v. 142, p. 269−285.

Plaziat, J.-C., Purser, B.H. and Philobbos, E. 1990. Seismic deformation structures (seismites) in the syn-rift sediments of the NW Red Sea (Egypt). Bulletin de la Société Géologique de France, v. 8, p. 419−434.

Potter, D. and St. Onge, A. 1991. Minton Pool, south-central Saskatchewan: a model for the basement induced structural and stratigraphic relationships. In: Sixth Williston Basin Symposium. J.E. Christopher and F.M. Haidl (eds.). Saskatchewan Geological Society, Special Publication 11, p. 21−33.

Pratt, B.R. 1994. Seismites in Mesoproterozoic Altyn Formation (Belt Supergroup), Montana: a test for tectonic control of peritidal carbonate cyclicity. Geology, v. 22, p. 1091–1094.

Pratt, B.R. 1998a. Syneresis cracks: subaqueous shrinkage in argillaceous sediments caused by earthquake-induced dewatering. Sedimentary Geology, v. 117, p. 1–10.

Pratt, B.R. 1998b. Molar-tooth structure in Proterozoic carbonate rocks: origin from synsedimentary earthquakes, and implications for the nature and evolution of basins and marine sediments. Geological Society of America Bulletin, v. 110, p. 1028–1045.

Pratt, B.R. 2001a. Septarian concretions: internal cracking caused by synsedimentary earthquakes. Sedimentology, v. 48, p. 189−213.

Pratt, B.R. 2001b. Oceanography, bathymetry and syndepositional tectonics of a Precambrian intracratonic basin: integrating sediments, storms, earthquakes and tsunamis in the Belt Supergroup (Helena Formation, c. 1.45 Ga), western North America. Sedimentary Geology, v. 141–142, p. 371−394.

Pratt, B.R. and Haidl, F.M. 2008. Microbial patch reefs in Upper Ordovician Red River strata, Williston Basin, Saskatchewan: signal of heating in a deteriorating epeiric sea. In: Dynamics of Epeiric Seas. B.R. Pratt, and C. Holmden (eds.). Geological Association of Canada, Special Paper 48, p. 315−352.

Rodríguez-López J. P., Meléndez, N., Soria, A. R., Luis Liesa, C. and Van Loon, A.J. 2007. Lateral variability of ancient seismites related to differences in sedimentary facies (the synrift Escucha Formation, mid-Cretaceous, eastern Spain). Sedimentary Geology, v. 201, p. 461–484.

Rossetti D.F. and Góes A.M. 2000. Deciphering the sedimentological imprint of paleoseismic events: an example from the Aptian Codó Formation, northern Brazil. Sedimentary Geology 135, 137–56

Seilacher, A. 1984. Sedimentary structures tentatively attributed to seismic events. Marine Geology, v. 55, p. 1–12.

Sims, J.D. 1973. Earthquake induced structures in sediments of Van Norman Lake, San Fernando, California. Science v. 182, p. 161–163.

Simms, M.J. 2007. Uniquely extensive soft-sediment deformation in the Rhaetian of the UK: evidence for earthquake or impact?. Palaeogeography, Palaeoclimatology, Palaeoecology, v. 244, p. 407−423.

Urban, M. and Qing, H. 2007. Preliminary core description and lithofacies analysis of the Ordovician Coronach Member, Herald Formation, southeastern Saskatchewan. In: Summary

of Investigations 2007, Saskatchewan Geological Survey, Saskatchewan Industry and Resources, Miscellaneous Report 2007-4.1, Paper A-3.

Warren, J.K. 2006. Evaporites: Sediments, Resources and Hydrocarbons. Springer, Berlin, 1035 pp.

Weidlich, O. and Bernecker, M. 2004. Quantification of depositional changes and paleo-seismic activities from laminated sediments using outcrop data. Sedimentary Geology, v. 166, p. 11−20.

APPENDICES

THIN SECTIONS

Thin section	Well Coordinates	Sample Depth (m)	Stratigraphic occurrence (member)	Deformation style		
				Brittle (Dolomudstone)	Soft (Dolomudstone)	Soft (Anhydrite)
1	12-02-07-11	2559	Upper Lake Alma			√
2	11-17-03-21	2805.3	Upper Lake Alma		√	√
3	06-18-06-10	2639.7	Upper Lake Alma			√
4	15-09-02-14	3030	Upper Coronach			√
5	15-09-02-14	3030	Upper Coronach			√
6	15-09-02-14	3046.1	Upper Lake Alma		√	
7	14-26-06-11	2550.2	Upper Coronach	√		
8	06-18-06-10	2619.2	Upper Coronach		√	
9	12-02-07-11	2561	Upper Lake Alma			√
10	12-02-07-11	2561	Upper Lake Alma			√
11	10-25-01-15	3115.6	Upper Coronach		√	
12	16-36-01-18	3051.65	Basal Lake Alma		√	
13	11-14-02-09	2965.1	Lower Lake Alma		√	
14	06-18-06-10	2645.7	Lower Lake Alma		√	
15	06-18-06-10	2634	Upper Lake Alma		√	√
16	12-02-07-11	2560	Upper Lake Alma			√
17	02-10-01-21	2959.8	Lower Lake Alma		√	
18	13-08-04-22	2776.7	Lower Lake Alma	√		
19	11-17-03-21	2808.5	Lower Lake Alma		√	
20	11-17-03-21	2808.5	Lower Lake Alma		√	
21	12-02-07-11	2560	Upper Lake Alma			√
22	06-18-06-10	2643.4	Lower Lake Alma		√	
23	10-25-01-15	3111.85	Upper Coronach		√	
24	10-25-01-15	3111.85	Upper Coronach		√	
25	06-18-06-10	2622.5	Upper Coronach		√	
26	06-18-06-10	2622.5	Upper Coronach		√	
27	15-09-02-14	3047.6	Upper Lake Alma			√
28	15-09-02-14	3047.6	Upper Lake Alma			√
29	15-09-02-14	3049.8	Upper Lake Alma			√
30	15-09-02-14	3032.8	Upper Coronach		√	
31	10-25-01-15	3135.7	Lower Lake Alma	√		
32	01-14-01-17	3073.6	Basal Coronach *	√	√	
33	15-09-02-14	3047.7	Basal Coronach *	√	√	
34	10-25-01-15	3112.6	Upper Coronach			√
35	10-25-01-15	3112.6	Upper Coronach			√
36	06-18-06-10	2641.8	Lower Lake Alma		√	
37	15-09-02-14	3048.3	Upper Lake Alma			√
38	15-09-02-14	3048.3	Upper Lake Alma			√
39	10-25-01-15	3130	Upper Lake Alma			√
40	10-25-01-15	3130	Upper Lake Alma			√
41	14-26-06-11	2569.3	Upper Lake Alma			√
42	14-26-06-11	2564.9	Upper Lake Alma		√	
43	14-26-06-11	2568.3	Upper Lake Alma			√
44	06-18-06-10	2614.2	Upper Coronach		√	
45	06-18-06-10	2640.15	Lower Lake Alma	√		
46	06-18-06-10	2622	Upper Coronach	√		
47	14-26-06-11	2553.65	Upper Coronach		√	
48	10-25-01-15	3134.6	Lower Lake Alma		√	

49	10-25-01-15	3116.3	Upper Coronach		√	
50	14-26-06-11	2571	Lower Lake Alma	√	√	
51	16-36-01-18	3051.65	Basal Lake Alma		√	
52	01-16-09-23	2473.2	Lower Lake Alma	√	√	
53	14-26-06-11	2563.5	Basal Coronach *		√	
54	14-26-06-11	2563.5	Basal Coronach *		√	

PUBLICATION